varies approximately inversely with axial ratio (for modest axial ratios).[1-3] Although theories of the behavior of nonelectrolyte rods do not strictly apply to solutions of charged particles, DNA molecules in aqueous solution can be treated in some contexts as "scaled" spherocylindrical rods with an effective radius dependent on the distance from the DNA surface required for the electrostatic repulsion potential to drop to $kT/2$.[4a]

We were able to fit the DNA concentrations at the observed isotropic/biphasic and biphasic/cholesteric phase boundaries at 20 or 70 °C to volume fractions predicted by Flory's theory with a single effective radius. The best-fit radii obtained at the two temperatures agreed well with the effective radii obtained for more dilute DNA solutions at a similar Na^+ concentration by sedimentation equilibrium[4a] and with the effective radius calculated from Poisson-Boltzmann statistics.[4b,d] Since electrostatic repulsion is the greatest obstacle to close packing of DNA molecules in solution, one expects that increasing ionic strength will cause a decrease in effective DNA radius and an increase in the critical DNA concentration necessary for liquid crystalline phase formation. Observations of Brian et al.[4a] were consistent with this prediction. A preliminary phase diagram for isotropic to cholesteric transitions in DNA solutions of high ionic strength (ca. 2 M) was described by Rill.[6b] The biphasic region at this sodium concentration was shifter toward higher DNA concentrations by about 60 mg/mL in comparison to the phase diagram presented in this paper. Previous studies also demonstrated an approximate inverse relationship between DNA length and the critical concentration at the isotropic/biphasic boundary.[6a] Together these results show that the isotropic to cholesteric phase transitions of DNA can be treated, to a first approximation, in terms of scaled particles within the context of the lattice statistics formalism of Flory and co-workers.[2a,b]

The unusual dependence of the ^{31}P line width on DNA concentration at concentrations above the fully cholesteric range can be interpreted most simply in terms of formation of a more highly ordered phase. This transition occurred abruptly over a narrow range of DNA concentrations, suggesting that major changes in DNA organization can occur readily despite the high macroscopic viscosities of these solutions. DNA concentrations occurring in vivo commonly approach or exceed those examined here, and the critical concentrations required for rodlike polymer phase transitions decrease with increasing length. As pointed out by Flory,[2a] the behavior of long, semiflexible polymers is expected to be intrinsically similar to that of shorter, rodlike analogues. The ready ability of rodlike DNA molecules to assume alternate liquid crystalline forms may, therefore, be of significance to mechanisms of DNA packing in vivo.

Acknowledgment. We are grateful to Dr. Penny Gilmer for use of her Leitz microscope and to Drs. Timothy Cross, Robert Fulton, and Theodore Williams for reading the manuscript and discussion.

Wavelength-Dependent Primary Photoprocesses of $Os_3(CO)_{12}$ in Fluid Solution and in Rigid Alkane Glasses at Low Temperature: Spectroscopic Detection, Characterization, and Reactivity of Coordinatively Unsaturated $Os_3(CO)_{11}$

James G. Bentsen and Mark S. Wrighton*

Contribution from the Department of Chemistry, Massachusetts Institute of Technology, Cambridge, Massachusetts 02139. *Received July 8, 1986*

Abstract: Wavelength-dependent photochemistry is reported for $Os_3(CO)_{12}$ in hydrocarbon solutions at 298 and 195 K and in rigid hydrocarbon glasses at 90 K. Near-UV and vis irradiation of 0.2 mM $Os_3(CO)_{12}$ at 298 K in alkane solutions containing 5 mM L yields mainly $Os_3(CO)_{11}L$ (L = PPh_3, $P(OMe)_3$) as the initial photoproduct with a wavelength-dependent quantum yield: $\Phi_{436nm} < 0.0001$, $\Phi_{366nm} = 0.017 \pm 0.001$, and $\Phi_{313nm} = 0.050 \pm 0.003$ for L = PPh_3, independent of the presence of added 0.1 M tetrahydrofuran. Photosubstitution of PPh_3 for CO is not affected by added 1 M CCl_4, and the 366 nm quantum yield does not change on increasing the PPh_3 concentration to 0.10 M, consistent with photodissociative loss of CO from an upper level excited state. Electronic spectral features for $Os_3(CO)_{12}$ become well-resolved in an alkane glass of 90 K; low-energy excitation into the first (382 nm: $10a_1' \rightarrow 16e'$; $^1A_1' \rightarrow {}^1E'$) or second (320 nm: $15e' \rightarrow 6a_2'$; $^1A_1' \rightarrow {}^1E'$) absorptions for $Os(CO)_{12}$ yields no net photochemistry in the 90 K alkane glass. However, excitation into the third electronic absorption (278 sh nm: $14e' \rightarrow 6a_2'$; $^1A_1' \rightarrow {}^1E'$) of 0.1 mM $Os_3(CO)_{12}$ yields loss of one CO as the only FTIR detected photoreaction to yield a single product, formulated as axially vacant $Os_3(CO)_{11}$ on the basis of FTIR and UV-vis spectral characterization and reaction chemistry. While the photogenerated $Os_3(CO)_{11}$ reacts with ^{13}CO at low temperature to give the axial-^{13}CO-$Os_3(CO)_{11}(^{13}CO)$, UV irradiation of axial-^{13}CO-$Os_3(CO)_{11}(^{13}CO)$ in a 90 K methylcyclohexane glass yields dissociative CO loss in a ratio of $^{12}CO/^{13}CO$ of greater than 28. These results suggest photodissociative loss of equatorial CO from $Os_3(CO)_{12}$, followed by rearrangement of equatorially vacant $Os_3(CO)_{11}$ to the axially vacant form. Photogenerated $Os_3(CO)_{11}$ reacts with two electron donor ligands to yield $Os_3(CO)_{11}L$ complexes (L = N_2, C_2H_4, PPh_3, 1-pentene, 2-MeTHF) and with H_2 to yield $H_2Os_3(CO)_{11}$. The $H_2Os_3(CO)_{11}$ complex has been detected by FTIR as an intermediate in the direct photoconversion ($\Phi_{366nm} = 0.02$) of $Os_3(CO)_{12}$ to $H_2Os_3(CO)_{10}$ in H_2-saturated alkane solutions at 298 K. Near-UV irradiation of $H_2Os_3(CO)_{11}$ cleanly yields $H_2Os_3(CO)_{10}$ and free CO at 298 or 90 K. Selective excitation into the second absorption of $Os_3(CO)_{12}$ at 90 K yields inefficient associative photosubstitution of strong π-acceptors (C_2H_4, C_5H_{10}, ^{13}CO) but not N_2 or 2-MeTHF for CO. In fluid solutions, competitive photofragmentation is correlated with long wavelength irradiation and with strong π-acceptor ligands (CO, C_2H_4, not PPh_3).

We report here a detailed characterization of the electronic, structural, and chemical properties of photogenerated, coordinatively unsaturated $Os_3(CO)_{11}$. The $Os_3(CO)_{11}$ can be photogenerated in rigid alkane glasses at low temperature according to eq 1. This article includes a detailed investigation of the wavelength dependent competition between dissociative CO loss

0002-7863/87/1509-4518$01.50/0

$$Os_3(CO)_{12} \xrightarrow[\text{alkane}]{h\nu,\ 90\ K} Os_3(CO)_{11} + CO \qquad (1)$$

and either associative photosubstitution of strong π-acceptor/weak σ-donor ligands for CO on $Os_3(CO)_{12}$ at 90 K or photofragmentation in fluid solution at 195 K. The dissociative loss of CO from mononuclear species upon photoexcitation has been very useful in unravelling mechanistic and electronic spectral features associated with mononuclear complexes.[1-4] While the photochemical reactivity of metal carbonyl cluster complexes has enabled the synthesis of new metal clusters,[5-7] new mononuclear metal carbonyl derivatives,[7-11] and intermediates providing entry into catalytic cycles for organic transformations,[7,12] few detailed mechanistic studies[13-18] exist. We have thus initiated investigations (i) to better understand and control factors affecting low-temperature photochemical generation of electron deficient polynuclear metal carbonyl complexes via dissociative ligand loss or metal framework rearrangement and (ii) to understand the electronic, structural, and reactivity properties of accumulated intermediates.

We report in a companion paper[19] a low-temperature photochemical investigation of the related $Ru_3(CO)_{12}$ and $Fe_3(CO)_{12}$ complexes. Results presented in this and the accompanying paper serve to demonstrate the ability to generate and characterize new electron deficient metal carbonyl cluster complexes by using photochemical techniques.[20] Our current findings suggest that it is possible to accumulate and characterize high nuclearity intermediates important in understanding reactions of clusters and surfaces.[21]

A problem which has limited thorough investigation of cluster chemistry is that high temperatures are often required to effect rate-limiting ligand loss or metal–metal bond cleavage.[22] Such high temperatures typically preclude accumulation of all but the thermodynamically favored pyrolysis product, and cluster fragmentation often competes with desired cluster based ligand transformations. Most approaches (we reference some examples involving osmium carbonyl clusters) therefore aim to provide enhanced reactivity for coordinatively saturated clusters via the initial replacement of CO by a labile ligand,[23] through associative pathways such as ligation of a reactive metal–metal bond with a bridging heteroatom(s),[24] direct attack with oxidizing agents[25] or strong nucleophiles such as hydroxide ion[26] and amines[27] on coordinated CO, electron-transfer catalysis,[28] or promotion of CO insertion into the metal–carbon bond of a bridging methylene.[29]

(1) Turro, N. J. *Modern Molecular Photochemistry*; Benjamin Cummings: Menlo Park, CA, 1978.

(2) Geoffroy, G. L.; Wrighton, M. S. *Organometallic Photochemistry*; Academic Press: New York, 1979.

(3) Publications representative of groups currently active in this area include the following: (a) Mitchener, J. C.; Wrighton, M. S. *J. Am. Chem. Soc.* **1983**, *105*, 1065–1067. (b) Turner, J. J.; Poliakoff, M. *ACS Symp. Ser.* **1983**, *211*, 35–37. (c) Sweany, R. L. *J. Am. Chem. Soc.* **1985**, *107*, 2374–2379. (d) Gerhartz, W.; Ellerhorst, G.; Dahler, P.; Eilbracht, P. *Liebigs Ann. Chem.* **1980**, 1296–1306. (e) Church, S. P.; Grevels, F.-W.; Hermann, H.; Schaffner, K. *Inorg. Chem.* **1985**, *24*, 418–422. (f) Welch, J. A.; Peters, K. S.; Vaida, V. *J. Phys. Chem.* **1982**, *86*, 1941–1947. (g) Hooker, R. H.; Rest, A. J. *J. Organomet. Chem.* **1983**, *249*, 137–147. (h) Fletcher, T. R.; Rosenfeld, R. N. *J. Am. Chem. Soc.* **1985**, *107*, 2203–2212. (i) Sedar, T. A.; Church, S. P.; Ouderkirk, A. J.; Weitz, E. *J. Amer. Chem. Soc.* **1985**, *107*, 1432–1433. (j) Lewis, K. E.; Golden, D. M.; Smith, G. P. *J. Am. Chem. Soc.* **1984**, *106*, 3905–3912. (k) Kelly, J. M.; Long, C.; Bonneau, R. *J. Phys. Chem.* **1983**, *87*, 3344–3349. (l) Miller, M. E.; Grant, E. R. *J. Am. Chem. Soc.* **1984**, *106*, 4635–4636. (m) Tumas, W.; Gitlin, B.; Rosan, A. M.; Yardley, J. T. *J. Am. Chem. Soc.* **1982**, *104*, 55–59. (n) Breckenridge, W. H.; Sinai, N. *J. Phys. Chem.* **1981**, *85*, 3557–3560. (o) Tyler, D. R.; Petrylak, D. P. *J. Organomet. Chem.* **1981**, *212*, 389–396. (p) Krusic, P. J.; Briere, R.; Rey, P. *Organometallics* **1985**, *4*, 801–803.

(4) (a) Burdett, J. K.; Turner, J. J. In *Cryochemistry*; Moskovits, M., Ozin, G. A., Eds.; Wiley: New York, 1976; pp 493–525. (b) Turner, J. J. In *Matrix Isolation Spectroscopy*; Barnes, A. J. et al., Eds.; **1982**, pp 495–515.

(5) (a) Adams, R. D.; Horwith, I. T.; Kim, H.-S. *Organometallics* **1984**, *3*, 548–552. (b) Adams, R. D.; Manning, D.; Segmuller, B. E. *Organometallics* **1983**, *2*, 149–153. (c) Adams, R. D.; Dawoodi, Z. *J. Am. Chem. Soc.* **1981**, *103*, 6510–6512. (d) Bhaduri, S.; Johnson, B. F. G.; Kelland, J. W.; Lewis, J.; Raithby, P. R.; Rehani, S.; Sheldrick, G. M.; Wang, K. *J. Chem. Soc., Dalton Trans.* **1979**, 562–568. (e) Heveldt, P. F.; Johnson, B. F. G.; Lewis, J.; Raithby, P. R.; Sheldrick, G. M. *J. Chem. Soc., Chem. Commun.* **1978**, 340–341. (f) Bentsen, J. G.; Wrighton, M. S. *Inorg. Chem.* **1984**, *23*, 512–515. (g) Leopold, D. G.; Vaida, V. *J. Am. Chem. Soc.* **1983**, *105*, 6809–6811. (h) Burkhardt, E. W.; Geoffroy, G. L. *J. Organomet. Chem.* **1980**, *198*, 179–188.

(6) Cullen, W. R.; Harbourne, D. A. *Inorg. Chem.* **1970**, *9*, 1839–1843.

(7) Austin, R. G.; Paonessa, R. S.; Giordano, P. J.; Wrighton, M. S. *Adv. Chem. Ser.* **1978**, *168*, 189–214.

(8) (a) Johnson, B. F. G.; Lewis, J.; Twigg, M. V. *J. Organomet. Chem.* **1974**, *67*, C75–C76. (b) Johnson, B. F. G.; Lewis, J.; Twigg, M. V. *J. Chem. Soc., Dalton Trans.* **1975**, 1876–1879.

(9) (a) Grevels, F.-W.; Renvers, J. G. A.; Takats, J. *Angew. Chem., Int. Ed. Engl.* **1981**, *20*, 452–460. (b) Doi, Y.; Yano, K. *Inorg. Chim. Acta* **1983**, *76*, L71–L73. (c) Yarrow, P.; Ford, P. C. *J. Organomet. Chem.* **1981**, *214*, 115–118.

(10) (a) Burke, M. R.; Takats, J.; Grevels, F.-W.; Renvers, J. G. A. *J. Am. Chem. Soc.* **1983**, *105*, 4092–4093. (b) Vioget, P.; Bonivento, M.; Roulet, R.; Vogel, P. *Helv. Chim. Acta* **1984**, *67*, 1630–1637.

(11) (a) Liu, D. K.; Wrighton, M. S.; McKay, D. R.; Maciel, G. E. *Inorg. Chem.* **1981**, *23*, 212–220. d) Liu, D. K.; Wrighton, M. S. *J. Am. Chem. Soc.* **1982**, *104*, 898–901.

(12) (a) Bamford, C. H.; Mahmud, M. V. *J. Chem. Soc., Chem. Commun.* **1972**, 762–763. (b) Graff, J. L.; Sanner, R. D.; Wrighton, M. S. *J. Am. Chem. Soc.* **1979**, *101*, 273–275. (c) Graff, J. L.; Wrighton, M. S. *J. Am. Chem. Soc.* **1980**, *102*, 2123–2125. (d) Graff, J. L.; Sanner, R. D.; Wrighton, M. S. *Organometallics* **1982**, *1*, 837–842. (e) Doi, Y.; Tamura, S.; Koshizuki, K. *J. Mol. Catal.* **1983**, *19*, 213–222. (f) Graff, J. L.; Wrighton, M. S. *Inorg. Chim. Acta* **1982**, *63*, 63–70. (g) Doi, Y.; Tamura, S.; Koshizuka, K. *Inorg. Chim. Acta* **1982**, *65*, L63–64.

(13) (a) Desrosiers, M. F.; Wink, D. A.; Ford, P. C. *Inorg. Chem.* **1985**, *24*, 1–2. (b) Desrosiers, M. F.; Ford, P. C. *Organometallics* **1982**, *1*, 1715–1716. (c) Desrosiers, M. F.; Wink, D. A.; Trautman, R.; Friedman, A. E.; Ford, P. C. *J. Am. Chem. Soc.* **1986**, *108*, 1917–1927.

(14) (a) Bock, C. R.; Wrighton, M. S. *Inorg. Chem.* **1977**, *16*, 1309–1313. (b) Geoffroy, G. L.; Epstein, R. A. *Inorg. Chem.* **1977**, *16*, 2795–2799. (c) Graff, J. L.; Wrighton, M. S. *J. Am. Chem. Soc.* **1981**, *103*, 2225–2231. (d) Graff, J. L.; Wrighton, M. S. *J. Am. Chem. Soc.* **1980**, *102*, 2123–2125. (e) Foley, H. C.; Geoffroy, G. L. *J. Am. Chem. Soc.* **1981**, *103*, 7176–7180.

(15) Epstein, R. A.; Gaffney, T. R.; Geoffroy, G. L.; Gladfelter, W. L.; Henderson, R. S. *J. Am. Chem. Soc.* **1979**, *101*, 3847–3852.

(16) Grevels, F.-W.; Renvers, J. G. A.; Takats, J. *J. Am. Chem. Soc.* **1981**, *103*, 4069–4073.

(17) Malito, J.; Markiewicz, S.; Pöe, A. *Inorg. Chem.* **1982**, *21*, 4335–4338.

(18) Tyler, D. R.; Altobelli, M.; Gray, H. B. *J. Am. Chem. Soc.* **1980**, *102*, 3022–3024.

(19) Bentsen, J. G.; Wrighton, M. S., following paper in this issue.

(20) Recently, for $H_4Ru_4(CO)_{12}$, we reported in a preliminary communication the first direct evidence that loss of CO from a high nuclearity cluster compound can obtain upon photoexcitation to permit characterization of $H_4Ru_4(CO)_{11}$ at subambient temperatures: Bentsen, J. G.; Wrighton, M. S. *J. Am. Chem. Soc.* **1984**, *106*, 4041–4043.

(21) (a) Muetterties, E. L.; Krause, M. J. *Angew. Chem., Int. Ed. Engl.* **1983**, *22*, 135–148. (b) Muetterties, E. L.; Rhodin, T. N.; Band, E.; Brucker, C. F.; Pretzer, W. R. *Chem. Rev.* **1979**, *79*, 91–137. (c) Muetterties, E. L.; Wexler, R. M. *Surv. Prog. Chem.* **1983**, *10*, 62–128. (d) Pöe, A. *Chem. Br.* **1983**, *19*, 997–1003. (e) Vahrenkamp, H. *Adv. Organomet. Chem.* **1983**, *22*, 169–208. (f) Ugo, R.; Psaro, R. *J. Mol. Catal.* **1983**, *20*, 53–79.

(22) Connor, J. A. *Top. Curr. Chem.* **1977**, *71*, 71–110.

(23) Tachikawa, M.; Shapley, J. R. *J. Organometallic Chem.* **1977**, *124*, C19–C22.

(24) Adams, R. D.; Yang, L.-W. *J. Am. Chem. Soc.* **1983**, *105*, 235–240.

(25) (a) Lawson, R. J.; Shapley, J. R. *J. Am. Chem. Soc.* **1976**, *98*, 7433–7435. (b) Shapley, J. R.; Pearson, G. A.; Tachikawa, M.; Schmidt, G. E.; Churchill, M. R.; Hollander, F. J. *J. Am. Chem. Soc.* **1977**, *99*, 8064–8065.

(26) (a) Johnson, B. F. G.; Lewis, J.; Kilty, P. A. *J. Chem. Soc. A* **1968**, 2859–2864. (b) Gross, D. C.; Ford, P. C. *Inorg. Chem.* **1982**, *21*, 1702–1704.

(27) (a) Mayr, A.; Lin, Y. C.; Boag, N. M.; Kaesz, H. D. *Inorg. Chem.* **1982**, *21*, 1704–1706. (b) Kaesz, H. D.; Knobler, C. B.; Andrews, M. A.; van Buskirk, G.; Szostak, R.; Strouse, C. E.; Lin, Y. C.; Mayr, A. *Pure Appl. Chem.* **1982**, *54*, 131–143.

(28) Arewgoda, M.; Robinson, B. H.; Simpson, J. *J. Am. Chem. Soc.* **1983**, *105*, 1893–1903.

(29) (a) Morrison, E. D.; Steinmetz, G. R.; Geoffroy, G. L.; Fultz, W. C.; Rheingold, A. L. *J. Am. Chem. Soc.* **1983**, *105*, 4104–4105; **1984**, *106*, 4783–4789. (b) Morrison, E. D.; Geoffroy, G. L.; Rheingold, A. L.; Fultz, W. C. *Organometallics* **1985**, *48* 1413–1418.

Approaches aimed at generating electron-deficient clusters, while most attractive, have been limited to a small number of cluster based systems[30,31] by the inability to generate such complexes in a systematic manner under conditions which ensure their survival. The novel reaction chemistry associated with the stable electron-deficient $H_2Os_3(CO)_{10}$[31] and $[HRh(PR_3)_2]_n$ (n = 2–4)[32] complexes, however, serves to justify this approach to developing and understanding cluster chemistry.

Recently, we[33,34] and others[35] have developed the ability to *photochemically* generate and characterize new electron-deficient, dinuclear metal–carbonyl complexes at low temperature, suggesting the possibility of maximizing associative reactions of clusters under conditions which ensure the survival of resulting intermediates. The solution photochemistry of the intensely investigated[36] $Mn_2(CO)_{10}$, $(\eta^5\text{-}C_5H_5)_2Mo_2(CO)_6$, and $(\eta^5\text{-}C_5H_5)_2Fe_2(CO)_4$ complexes is consistent with the intermediacy of two different primary photoproducts: 17e⁻ mononuclear fragments and dinuclear CO loss products. Interestingly, light induced loss of CO from $Mn_2(CO)_{10}$[33] and *trans*-$(\eta^5\text{-}C_5R_5)_2Fe_2(CO)_4$ (R = H, $CH_2C_6H_5$, CH_3)[34,35] is the only net photoreaction in rigid media at low temperature, whereas net metal–metal bond cleavage is very important in fluid solution at 298K. Relatively little is known regarding the photochemistry of clusters containing three or more metal atoms.[20] Coordinatively unsaturated cluster fragments from $M_3(CO)_{12}$ (M = Ru, Os) complexes have been postulated as intermediates in the formation and transformation of organic substrates.[37] The high symmetry of $M_3(CO)_{12}$ complexes has made them attractive candidates for detailed electronic[38] and vibrational[39] analyses important to our fundamental photochemical studies.

Two laboratories[13,17] have interpreted the photofragmentation kinetics for $Ru_3(CO)_{12}$ in terms of intermediate formation of a nonradical reactive isomer of $Ru_3(CO)_{12}$ via excitation into the first allowed electronic absorption ($15e' \rightarrow 6a_2'$; $\sigma \rightarrow \sigma^*$). Only higher energy excitation is believed to yield competitive photosubstitution chemistry.[13] Near-UV irradiation of $Os_3(CO)_{12}$ in solution at 298K is known to lead to photosubstitution[18] of CO by PPh_3 while photofragmentation[8] of $Ru_3(CO)_{12}$ is a principal photochemical pathway in the presence of CO, C_2H_4, or PPh_3. The difference in reactivity between the Os (substitution) and Ru (fragmentation) species has been interpreted[18,40] in terms of an inversion of the relative ordering for the two lowest energy electronic excited states, while differences in the metal–metal bond strengths (Os–Os > Ru–Ru) may be the determining factor. More recently, however, the long wavelength photoactivity of $Os_3(CO)_{12}$ in the presence of olefins, to yield 1,2-diosmacyclobutane derivatives and $Os(CO)_4(\eta^2\text{-olefin})$ species, has been interpreted[10] as indicative of a common photochemical intermediate for $Os_3(CO)_{12}$ and $Ru_3(CO)_{12}$ clusters upon population of their lowest excited states.

Experimental Section

Instrumentation. UV–vis absorption spectra were recorded on a Cary 17 spectrophotometer or a Hewlett-Packard Model 8451 A diode array spectrophotometer. FTIR absorption spectra were recorded on a Nicolet 7199 or 60SX Fourier transform infrared spectrometer. Low-temperature IR spectra were obtained by using a Precision Cell, Inc. Model P/N 21.000 variable temperature dewar with CaF_2 outer windows, by using liquid N_2 or dry ice/acetone as coolant. Fluid hydrocarbon solutions were contained in a 1.0 or 0.2 mm pathlength cell with CaF_2 windows. A small hole drilled in the metal portion of the sample cell accommodates the junction end of a copper-constantin thermocouple. Temperatures are considered accurate to ±2 K at fixed temperature. All sample preparations were carried out under Ar or N_2 by using Vacuum Atmospheres He-63-P Drilab glove boxes with attached He-493 Dri-Train.

Irradiations. Photochemical reactions were carried out at 90 K by using a Bausch and Lomb SP 200-W high pressure Hg lamp (output filtered with 10 cm of H_2O to remove IR) or an H_2O-cooled Hanovia 450-W medium pressure Hg lamp. A quartz filter was used for broad band irradiations. The λ > 280-, 370-, or 420-nm irradiations were effected with Pyrex, Corning no. 0-51, or no. 3-73 glass filters, respectively. Quantum yields were measured in a merry-go-round[41] by using $\sim 10^{-4}$ M $Os_3(CO)_{12}$ and the appropriate ligand concentrations. Samples (3 mL) in 13 × 100 mm test tubes were freeze–pump–thaw degassed ($<10^{-5}$ torr, 3 cycles) and hermetically sealed prior to irradiation. The light source was a 550-W medium pressure Hg lamp (Hanovia) equipped with Corning glass filters to isolate the 366- or 436-nm Hg emissions. The 313-nm Hg emission was isolated with a chemical (K_2CO_3, 1 g L^{-1}/K_2CrO_4, 0.27 g L^{-1} solution) and glass (Corning no. 7-54) filter system. Ferrioxalate actinometry[42] was used to determine light intensities which were typically $<6 \times 10^{-8}$ einstein/min. Quantum yields were corrected to account for incomplete light absorption. Product distributions were determined by FTIR spectroscopy. "Flash photolysis" of the $Os_3(CO)_{12}$ was carried out by using a Xenon Corporation flash photolysis apparatus as a source. A 50-μs flash was used in order to minimize secondary photolysis.

Materials. The $Os_3(CO)_{12}$ (Strem) was used as received. The $P(OMe)_3$ (Aldrich) was distilled, and the PPh_3 (Aldrich) was recrystallized 3 times from EtOH. The photochemistry at low temperature was carried out by using 3-methylpentane (MP, Aldrich, 99+%), methylcyclohexane (MCH, J. T. Baker, Photorex grade), 2-methyltetrahydrofuran (2-MeTHF, Aldrich), and 1-pentene (99+%, Phillips). All solvents except 1-pentene were distilled over Na under Ar prior to use. The 1-pentene was passed through activated Al_2O_3 (neutral, Woelm) and degassed. Research grade CO, C_2H_4, N_2, and H_2 were obtained from Matheson. The ^{13}CO (99% ^{13}C, <4% ^{18}O) was obtained from Cambridge Isotope Laboratories.

Chemicals. The $Os_3(CO)_{11}(C_2H_4)$ and $Os_3(CO)_{11}(PPh_3)$ complexes were prepared according to literature procedures.[43] The $Os_3(CO)_{11}(PPh_3)$ complex was alternatively prepared under photochemical conditions[18] by near-UV irradiation (12 h with Pyrex and H_2O filtered emission from a Hanovia 450-W medium pressure Hg lamp) of $Os_3(CO)_{12}$ (300 mg) in a PPh_3-containing (435 mg) toluene (800 mL) solution at 330 K. Removal of toluene under reduced pressure yielded a yellow solid which was a mixture of $Os_3(CO)_{12-n}(PPh_3)_n$ (n = 0–3) complexes as determined by FTIR.[44,45] The $Os_3(CO)_{12}$ and $Os_3(CO)_{11}$-

(30) (a) Burgess, K.; Johnson, B. F. G.; Kaner, D. A.; Lewis, J.; Raithby, P. R.; Syed-Mustaffa, S. N. A. B. *J. Chem. Soc., Chem. Commun.* **1983**, 455–457. (b) Hay, C. M.; Johnson, B. F. G.; Lewis, J.; McQueen, R. C. S.; Raithby, P. R.; Sorrell, R. M.; Taylor, M. J. *Organometallics* **1985**, *4*, 202–204. (c) Balch, A. L.; Fossett, L. A.; Guimerans, R. R.; Olmsted, M. M. *Organometallics* **1985**, *4*, 781–788. (d) Frost, P. W.; Howard, J. A. K.; Spencer, J. L.; Turner, D. G.; Gregson, D. *J. Chem. Soc., Chem. Commun.* **1981**, 1104–1106. (e) Gregson, D.; Howard, J. A. K.; Murray, M.; Spencer, J. L. *J. Chem. Soc., Chem. Commun.* **1981**, 716–717. (f) Bertolucci, A.; Freni, M.; Romiti, P.; Ciani, G.; Sironi, A.; Albinati, A. *J. Organometallic Chem.* **1976**, *113*, C61–C64. (g) Ciani, G.; D'Alfonso, G. D.; Freni, M.; Roniti, P.; Sironi, A.; Albinati, A. *J. Organometallic Chem.* **1977**, *136*, C49–C51. (h) Wilson, R. D.; Bau, R. *J. Am. Chem. Soc.* **1976**, *98*, 4687–4689.

(31) (a) Deeming, A. J.; Hasso, S. *J. Organomet. Chem.* **1976**, *114*, 313–324. (b) Shapley, J. R.; Keister, J. B.; Churchill, M. R.; DeBoer, B. G. *J. Am. Chem. Soc.* **1975**, *97*, 4145–4146. (c) Deeming, A. J. In *Transition Metal Clusters*; Johnson, B. F. G., Ed.; Wiley: Chichester, 1980.

(32) (a) Sivak, A. J.; Muetterties, E. L. *J. Am. Chem. Soc.* **1979**, *101*, 4878–4887. (b) Kulzick, M.; Price, R. T.; Muetterties, E. L.; Day, V. W. *Organometallics* **1982**, *1*, 1256–1258. (c) Burch, R. R.; Shusterman, A. J.; Muetterties, E. L.; Teller, R. G.; Williams, J. M. *J. Am. Chem. Soc.* **1983**, *105*, 3546–3556.

(33) Hepp, A. F.; Wrighton, M. S. *J. Am. Chem. Soc.* **1983**, *105*, 5934–5935.

(34) (a) Hepp, A. F.; Blaha, J. P.; Lewis, C.; Wrighton, M. S. *Organometallics* **1984**, *3*, 174–177. (b) Blaha, J. P.; Bursten, B. E.; Dewan, J. C.; Frankel, R. B.; Randolph, C. L.; Wilson, B. A.; Wrighton, M. S. *J. Am. Chem. Soc.* **1985**, *107*, 4561–4562.

(35) Hooker, R. H.; Mahmoud, K. A.; Rest, A. J. *J. Chem. Soc., Chem. Commun.* **1983**, 1022–1024.

(36) Meyer, T. J.; Casper, J. V. *Chem. Rev.* **1985**, *85*, 187–218.

(37) (a) Johnson, B. F. G.; Lewis, J. *Adv. Inorg. Chem. Radiochem.* **1981**, *24*, 225–355. (b) Adams, R. D. *Acc. Chem. Res.* **1983**, *16*, 67–72. (c) Lewis, J.; Johnson, B. F. G. *Gazz. Chim. Ital.* **1979**, *109*, 271–289.

(38) Delley, B.; Manning, M. C.; Ellis, D. E.; Berkowitz, J.; Trogler, W. C. *Inorg. Chem.* **1982**, *21*, 2247–2253.

(39) Battiston, G. A.; Bor, G.; Dietler, U. K.; Kettle, S. F. A.; Rossetti, R.; Sbrignadello, G.; Stanghellini, P. L. *Inorg. Chem.* **1980**, *19*, 1961–1973.

(40) Tyler, D. R.; Levenson, R. A.; Gray, H. B. *J. Am. Chem. Soc.* **1978**, *100*, 7888–7893.

(41) Moses, F. G.; Liu, R. S. H.; Monroe, B. M. *Mol. Photochem.* **1969**, *1*, 245–249.

(42) Hatchard, C. G.; Parker, C. A. *Proc. R. Soc. London, Ser. A* **1956**, *235*, 518–536.

(43) Johnson, B. F. G.; Lewis, J.; Pippard, D. A. *J. Chem. Soc., Dalton Trans.* **1981**, 407–412.

(44) Trepathi, S. C.; Srivastava, S. C.; Mani, R. P.; Shrimal, A. K. *Inorg. Chim. Acta* **1975**, *15*, 249–290.

Table I. IR and UV–vis Data for Relevant Complexes[a]

species	temp, K	absorption maxima: ν, cm^{-1} (ϵ or rel od)	absorption maxima: λ, nm (ϵ or rel od)
$Os_3(CO)_{12}$	298	2069 (30 000), 2036 (31 000), 2015 (11 000), 2004 (9700)	385 sh (4200), 330 (10 800), 280 sh (11 100), 246 (29 300)
	90	2070 (45 000), 2064 (3800), 2035 (52 000), 2028 (3400), 2014 (17 000), 2000 (18 000)	381 (7200), 320 (26 000), 278 sh (16 000), 245 (43 000)
$Os_3(CO)_{11}$[b]	90	2114 (500), 2060 (21 000), 2051 (18 000), 2033 (9300), 2021 (33 000), 2011 (3200), 1996 (14 000), 1970 (2600)	524 (860), 358 (11 000), 300 (14 000), 280 sh (14 000), 269 sh (23 000), 260 (29 000), 232 sh (31 000)
$Os_3(CO)_{11}(N_2)$[b]	90	2237 (1200), 2115 (2600), 2066 (23 000), 2052 (24 000), 2031 (12 000), 2017 (25 000), 2011 (6900), 1995 (12 000), 1977 (970)	380 (6100), 322 (19 000), 282 (24 000), 269 (25 000), 248 (38 000), 221 (44 000)
$Os_3(CO)_{11}(C_2H_4)$	298	2117 (1100), 2065 (14 000), 2049 (11 000), 2029 (29 000), 2009 (4600), 2006 (7200), 1997 (4300), 1985 (1300), 1970 (2000)	
	90	2121 (2600), 2068 (26 000), 2049 (15 000), 2029 (37 000), 2010 (8500), 2005 (12 000), 1994 (7500), 1982 (2700), 1968 (4100)	
$Os_3(CO)_{11}$(2-MeTHF)	90[e]	2109 (1.0), 2055 (8.6), 2031 (8.6), 2012 (12), 1995 (4.3), 1978 (3.7), 1969 (4.6), 1950 (2.8), 1936 (3.1)	
$Os_3(CO)_{11}(^{13}CO)$ equil mixture[b]	90	2070 (20 000), 2064 (16 000), 2035 (25 000), 2029 (13 000), 2014 (8700), 2009 (6600), 2000 (11 000), 1990 (2400), 1969 (940), 1959 (1400)	
$Os_3(CO)_{11}(^{13}CO)$ axial[b]	90	2070 (16 000), 2064 (22 000), 2036 (6100), 2029 (29 000), 2015 (6100), 2009 (5400), 2000 (12 000), 1969 (1700)	
$Os_3(CO)_{11}(^{13}CO)$ equatorial[c]	90	2070 (23 000), 2065 (14 000), 2035 (40 000), 2014 (11 000), 2010 (7500), 2000 (9400), 1990 (4000), 1959 (2700)	
$H_2Os_3(CO)_{11}$[d]	298	2137 (1000), 2088 (9200), 2065 (13 000), 2057 (12 000), 2054 (12 000), 2029 (5900), 2018 (5100), 2000 (5100), 1986 (3300)	375 (6500), 324 (6200)
	90	2139 (1200), 2088 (12 000), 2064 (17 000), 2058 (12 000), 2053 (12 000), 2029 (5300), 2023 (6500), 2015 (6800), 1997 (4800), 1982 (3500)	368 (11 000), 327 (8500)
$H_2Os_3(CO)_{10}$	298	2112 (210), 2075 (14 600), 2063, (10 700), 2025 (23 000), 2010 (13 000), 1988 (2800), 1972 (250), 1957 (170)	553 (200), 327 (11 100), 287 (8500)
	90	2112 (300), 2075 (16 000), 2061 (12 000), 2023 (23 000), 2007 (12 000), 1988 (2800)	550 sh (700), 323 (22 000), 279 (16 000)

[a] All spectra are measured in methylcyclohexane unless noted otherwise; IR spectra are recorded at 2-cm^{-1} resolution and UV–vis data are accurate to ±2 nm. [b] Extinction coefficients estimated assuming clean conversion to a single product by digital subtraction of spectral features associated with unreacted $Os_3(CO)_{12}$. [c] Extinction coefficients estimated by digital subtraction of the 90 K spectral features for axial-^{13}CO-$Os_3(CO)_{11}(^{13}CO)$ from those obtained at 90 K for the equilibrium mixture of isoenergetic isomers. [d] Recorded in a CO-saturated solution. [e] Recorded in 2-MeTHF.

(PPh_3) complexes were extracted with 300 mL of hexane and chromatographed on a 250 mL by 5 cm bed of Florisil (60–100 mesh, MCB) to yield a single mobile yellow band of $Os_3(CO)_{11}(PPh_3)$. The $Os_3(CO)_{11}(PPh_3)$ was recrystallized from hexane/CH_2Cl_2 in 40% overall yield.

The $H_2Os_3(CO)_{10}$ complex[31] was prepared photochemically[7] in high yield as follows. A 500-mL, heavy-walled, round-bottomed flask was charged with $Os_3(CO)_{12}$ (1 g) and 300 mL of toluene under 1 atm of H_2. The closed vessel was subsequently heated with stirring to 330 K (dissolving the $Os_3(CO)_{12}$) and irradiated for 4 h with four General Electric Blacklight bulbs (355 ± 20 nm, $\sim 4 \times 10^{-6}$ einstein/min). The solution was purged briefly with H_2 at 330 K to remove photogenerated CO and was subsequently cooled to 293 K to precipitate most of the unreacted $Os_3(CO)_{12}$. After the purple supernatant was decanted, unreacted $Os_3(CO)_{12}$ was taken up in more toluene and irradiated under H_2 at 330 K as above. A second purple supernatant was combined with the first, and the resulting mixture was evaporated to dryness under reduced pressure to yield a purple solid determined by FTIR to contain predominantly $H_2Os_3(CO)_{10}$, some $Os_3(CO)_{12}$, and unidentified minor products. The $H_2Os_3(CO)_{10}$ was extracted with hexane and chromatographed on a silica gel (58 micron, Alfa) column with hexane as eluant. The $H_2Os_3(CO)_{10}$ eluted first as a purple band, closely followed by $Os_3(CO)_{12}$ (yellow). The $H_2Os_3(CO)_{10}$ was recrystallized from hexane as a purple solid in 88% overall yield.

$H_2Os_3(CO)_{11}$ was prepared[31] by charging a 50-mL, heavy-walled glass tube with $H_2Os_3(CO)_{10}$ (250 mg), hexane (30 mL), and 50 psi of CO. The solution turned from purple ($H_2Os_3(CO)_{10}$) to yellow ($H_2Os_3(CO)_{11}$) during 1 h at 298 K. The product was precipitated from solution at 195 K and found to dissolve only slowly on the time scale of subsequent rapid warmup to 298 K; the solvent was decanted in air at 298 K, and the remaining damp yellow powder was dried briefly (5 min) under vacuum before storing under N_2.

Photoreactions at 90 K. Deoxygenated alkane (3-methylpentane or methylcyclohexane) solutions containing ~0.1 mM $Os_3(CO)_{12}$ were exposed to Ar or a reactive gas (C_2H_4, CO, ^{13}CO, N_2, or H_2), loaded in the P/N 21.000 cell (~1.0-mm path length) under an atmosphere of Ar, and cooled to 90 K. Reactive gas solubilities at 1 atm in alkane media at 298 K were estimated from literature data:[46] [CO] = 0.01 M, [C_2H_4] = 0.05 M, [H_2] = 0.003 M, [N_2] = 0.004 M. The $Os_3(CO)_{12}$ concentration at 90 K was limited to ~0.1 mM; higher concentrations of complex yielded additional IR spectral features at 90 K, suggesting solute aggregation.

Results and Discussion

A. Dissociative Loss of CO From $Os_3(CO)_{12}$. (i) Photosubstitution Reactions at 298 K. The solution photochemistry for $Os_3(CO)_{12}$ demonstrates wavelength, temperature, and entering group effects on two net photoreactions: photosubstitution of CO and photofragmentation. Photosubstitution dominates for phosphine and phosphite entering groups. Two low-energy electronic absorption spectral features appear at 330 and 385 nm for $Os_3(CO)_{12}$ in fluid alkane solution at 298 K, Table I. These features overlap the tailing of higher energy electronic absorption features centered at 246 and 280 nm. Near-UV and vis irradiation of a 298 K isooctane solution of $Os_3(CO)_{12}$ (0.2 mM) and PPh_3 or $P(OMe)_3$ (5.0 mM) results in photosubstitution according to eq 2 with wavelength dependent quantum yields, Table IIa: Φ_{436nm}

$$Os_3(CO)_{12} \xrightarrow[L = PPh_3,\ P(OMe)_3]{h\nu,\ 298\ K,\ alkane} Os_3(CO)_{11}L + CO \qquad (2)$$

< 0.0001, Φ_{366nm} = 0.017 ± 0.001, and Φ_{313nm} = 0.050 ± 0.003,

(45) Deeming, A. J.; Johnson, B. F. G.; Lewis, J. *J. Chem. Soc. A* **1970**, 897–901.

(46) (a) Stephen, H.; Stephen, T. *Solubility of Inorganic and Organic Compounds*; Macmillan: New York, 1963. (b) Seidel, A.; Linke, W. F. *Solubilities of Inorganic and Metal Organic Compounds*, 4th ed.; D. van Nostrand Co.: Princeton, NJ.

Table II. Wavelength-Dependent Disappearance Rates for Photoexcited $Os_3(CO)_{12}$

a. Disappearance Quantum Yields for $Os_3(CO)_{12}$ in Isooctane at 298 K°

conditions	($\Phi \times 10^3$) 436 nm	366 nm	313 nm
5 mM PPh_3	<0.1	17 ± 1	50 ± 3
5 mM $P(OMe)_3$			52 ± 5
5 mM PPh_3, 100 mM THF	<0.1	17 ± 3	50 ± 5
100 mM PPh_3	<0.1	17 ± 3[b]	
3 mM H_2		20 ± 5[c]	

b. Normalized Disappearance Rates (% Decline) for 5 min of Pyrex-Filtered or Broad Band (Quartz) Irradiation of $Os_3(CO)_{12}$ at 90 K[d]

filter	normalized % decline[e] (a) MCH	(b) MP/N_2	(c) 2-MeTHF	(d) (MP/C_2H_4)	(e) 1-pentene
Pyrex[f]	<0.5	<0.5	<0.5	1.3 (2)	2.0 (4)
quartz	10 (2)	10 (2)	12 (2)	11 (2)	20 (4)

[a] $Os_3(CO)_{11}L$ (L = PPh_3, $P(OMe)_3$) is the only product detected unless otherwise specified. [b] $Os(CO)_4(PPh_3)$ also detected as a minor product along with $Os_3(CO)_{11}(PPh_3)$ (>95%). [c] $H_2Os_3(CO)_{10}$ is the product observed. [d] MCH = methylcyclohexane; MP = 3-methylpentane; 2-MeTHF = 2-methyltetrahydrofuran. The only product observed is $Os_3(CO)_{11}$ in a and $Os_3(CO)_{11}L$ (L = N_2, 2-MeTHF, C_2H_4, C_5H_{10}) in b–e. [e] Numbers in parentheses represent uncertainty in the least significant digit. [f] Pyrex transmits light $\lambda > 280$ nm.

respectively for L = PPh_3. The 313-nm quantum yield, corrected for weak overlapping absorption by the excess PPh_3, agrees with that obtained by using $P(OMe)_3$ (transparent at 313 nm) as the entering group. The same quantum yields are obtained with PPh_3 for such solutions containing 0.1 M tetrahydrofuran (THF). Added 1.0 M CCl_4 does not affect photosubstitution according to eq 2. When the PPh_3 concentration is increased to 0.10 M the 436- and 366-nm quantum yields for reaction according to eq 2 remain <0.0001 and 0.017 ± 0.003, respectively. The same reaction 2 occurs for 313-nm irradiation, but conversion is slow due to significant absorption at 313 nm by the excess PPh_3.

The quantum yield data at 366 and 313 nm support dissociative loss of CO from $Os_3(CO)_{12}$ at 298 K and suggest the intermediacy of $Os_3(CO)_{11}$ in the photosubstitution reaction according to eq 2. The inability of CCl_4, a possible radical trap, to affect the photochemistry of $Os_3(CO)_{12}$ in PPh_3-containing solutions is consistent with the conclusion that reactive diradical species, resulting from metal–metal bond homolysis are not important intermediates in the chemistry represented by eq 2. The wavelength dependence of the photosubstitution quantum yield rules out the previous suggestion[18] that the lowest allowed electronic excited state (responsible for 436-nm absorption at 298 K) alone controls the photochemistry of $Os_3(CO)_{12}$. Selective excitation into the second electronic absorption of $Os_3(CO)_{12}$ is not possible in fluid solution, due to strongly overlapping higher energy features. The wavelength dependence of the photosubstitution quantum yields suggests, however, that unavoidable excitation of these higher energy features may, in fact, account for the 366-nm photosubstitution behavior observed with PPh_3 at 298 K.

(ii) Photogeneration of $Os_3(CO)_{11}$ in Alkane Media at 90 K. The overlapping electronic spectral features for $Os_3(CO)_{12}$ become better resolved on cooling from 298 to 90 K in hydrocarbon media.[40] The two low-energy features both sharpen significantly on cooling, and the more intense 330-nm feature blue-shifts to 320 nm. The higher energy features sharpen significantly on cooling, resulting in nearly complete decline of their contribution to the electronic spectral absorptions at $\lambda > 300$ nm. These changes enable selective excitation of individual electronic transitions for $Os_3(CO)_{12}$ at 90 K. Importantly, for $Os_3(CO)_{12}$ in an Ar- or N_2-containing MCH glass or an Ar-containing MP glass at 90 K, selective excitation into the spectroscopically resolved first and second electronic absorptions with $\lambda > 370$-nm or $\lambda =$ 313-nm irradiation, respectively, does not yield photochemistry. Additional excitation into the low-energy tail of the third electronic absorption with $\lambda > 280$-nm irradiation yields clean FTIR and UV–vis spectral changes (Figure 1 (parts a and b) for irradiation in an N_2-containing MCH glass) consistent with slow conversion of $Os_3(CO)_{12}$ to $Os_3(CO)_{11}$ (Table I) and free CO (2132 cm^{-1}). These results suggest CO loss is associated with excitation into the third electronic absorption of $Os_3(CO)_{12}$. The wavelength dependent accumulation of $Os_3(CO)_{11}$ at 90 K appears to correlate with the photosubstitution efficiencies observed in fluid solution at 298 K.

Warmup to 298 K of a 90 K MCH glass containing photogenerated $Os_3(CO)_{11}$ and excess PPh_3 results in essentially quantitative conversion of all photogenerated $Os_3(CO)_{11}$ to $Os_3(CO)_{11}(PPh_3)$. Spectral data supporting this claim are presented as Supplementary Material. Warmup of $Os_3(CO)_{11}$ in the presence of equal amounts (10 mM) of PPh_3 and CCl_4 yields $Os_3(CO)_{11}(PPh_3)$. Similar warmup to 195 K in the presence of THF yields $Os_3(CO)_{11}$(THF). The $Os_3(CO)_{11}$(THF) complex reacts with subsequently added PPh_3 to yield $Os_3(CO)_{11}(PPh_3)$. Clearly, the intermediacy of $Os_3(CO)_{11}$ can account for the 298 K photosubstitution behavior of $Os_3(CO)_{12}$.

We now consider the characterization of $Os_3(CO)_{11}$ in detail. For the near-UV irradiation of ~0.1 mM $Os_3(CO)_{12}$ in a N_2-containing methylcyclohexane (MCH) glass at 90 K (Figure 1, parts a and b), absorbance changes occur in constant ratio to ~100% conversion and are persistent for several hours in the dark at 90 K. The key IR spectral changes are decline of absorption features attributed to $Os_3(CO)_{12}$, growth of a band at 2132 cm^{-1} associated with free CO in the glass,[47] and growth of a number of bands in the region where $Os_3(CO)_{12}$ absorbs. UV–vis spectral changes also occur and show a decline in absorbance of the intense absorptions at 320 and 381 nm of $Os_3(CO)_{12}$, growth of an intense electronic transition at 358 nm, and growth of a weak, low-energy, absorption centered at 524 nm. The 2132-cm^{-1} feature in the IR establishes that loss of CO occurs from photoexcited $Os_3(CO)_{12}$. The absorptivity of free CO was determined independently at 90 K by measuring the absorptivity at 2132 cm^{-1} for known fractional light-induced conversion of $Cr(CO)_6$ or $W(CO)_6$ to CO and the appropriate $M(CO)_5$ fragment; the values of ϵ_{CO} (M^{-1} cm^{-1}) from these precursors (~400 ± 10% in MCH or MP; ~350 ± 15% in 2-methyltetrahydrofuran (2-MeTHF); ~370 ± 15% in 1-pentene) are consistent with a previous report.[48] Within experimental error, the amount of free CO detected in Figure 1b is consistent with the appearance of one CO for every $Os_3(CO)_{12}$ consumed. The photoproduct is thus formulated as $Os_3(CO)_{11}$, eq 1. The weak, low-energy, 524-nm feature [ϵ = 860 M^{-1} cm^{-1} assuming conversion to a single product] is consistent with formation of a coordinatively unsaturated product. The intense 358-nm feature suggests retention of the trinuclear metal framework.

The IR spectral features attributed to $Os_3(CO)_{11}$, Table I, establish an all terminal undecacarbonyl ligand set and an axial vacancy. $Os_3(CO)_{11}L$ complexes (L = $2e^-$ donor ligands) have been structurally characterized by crystallography and/or ^{13}C NMR and exist in one of two all terminal ligand set geometries related to the D_{3h} structure of $Os_3(CO)_{12}$[49] by replacement of an axial or an equatorial (in the plane defined by the trinuclear metal framework) CO ligand by L. These two undecacarbonyl ligand set geometries [e.g., axial L = CNMe,[43] NCMe,[43,50] NC_5H_5;[43] equatorial L = C_2H_4,[43] *cis*- and *trans*-$CF_3(H)CC(H)CF_3$,[51] $P(OMe)_3$[43,52]] have characteristic IR signatures in the CO stretching region which enable a clear distinction between the two classes of $Os_3(CO)_{11}L$ complexes. This distinction is evident from com-

(47) Leroi, G. E.; Ewing, G. E.; Pimentel, G. C. *J. Chem. Phys.* **1964**, *40*, 2298–2303.
(48) Pope, K. R.; Wrighton, M. S. *Inorg. Chem.* **1985**, *24*, 2792–2796.
(49) Churchill, M. R.; DeBoer, B. G. *Inorg. Chem.* **1977**, *16*, 878–884.
(50) Dawson, P. A.; Johnson, B. F. G.; Lewis, J.; Puga, J.; Raithby, P. R.; Rosales, M. J. *J. Chem. Soc., Dalton Trans.* **1982**, 233–235.
(51) Dawoodi, Z.; Henrick, K.; Mays, M. J. *J. Chem. Soc., Chem. Commun.* **1982**, 696–698.

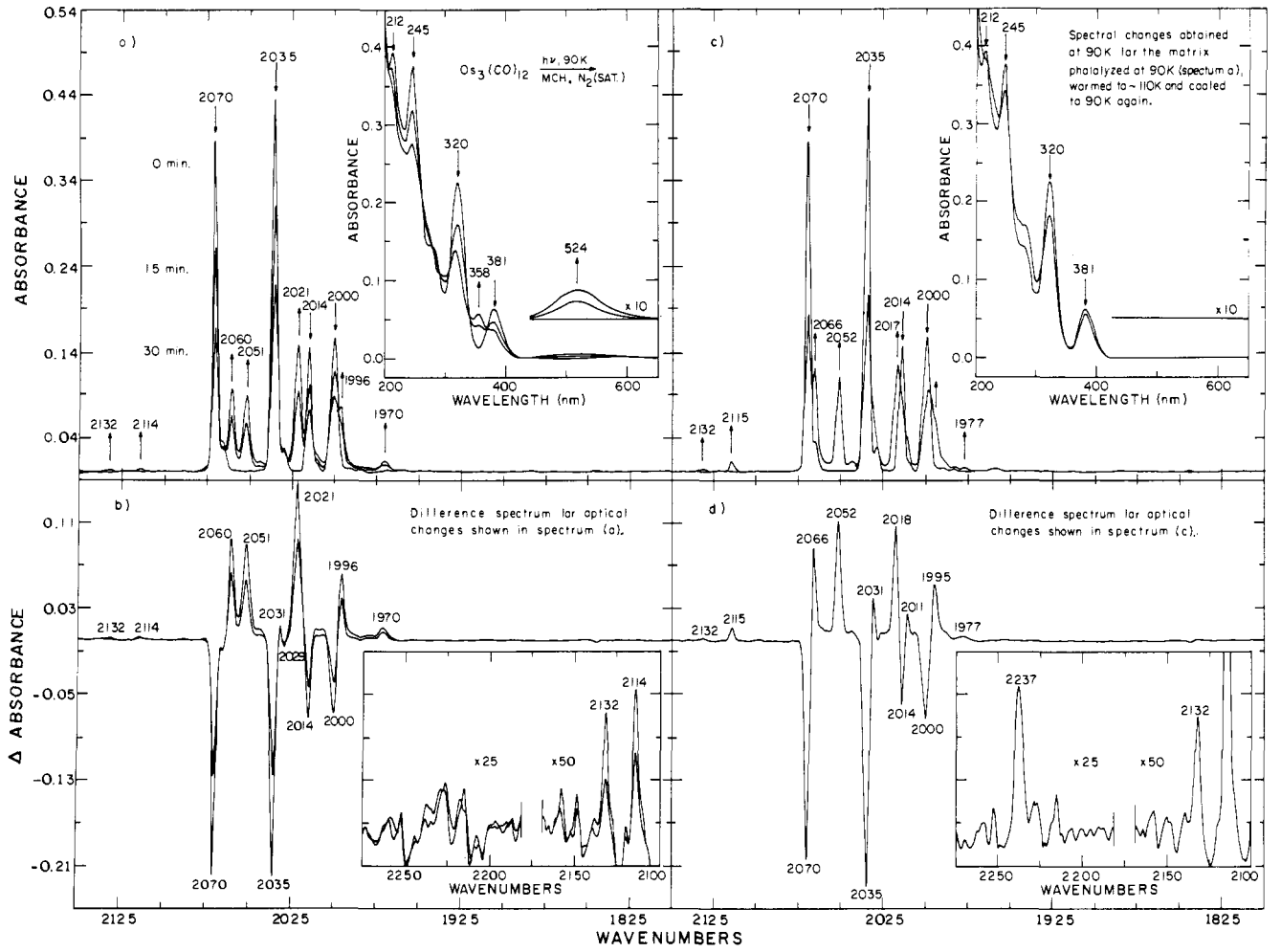

Figure 1. (a) IR and UV–vis (inset) spectral changes and (b) associated IR difference spectrum accompanying near-UV irradiation of 0.1 mM $Os_3(CO)_{12}$ in a N_2-containing MCH glass at 90 K. The band at 2132 cm^{-1} (spectrum b, inset) is attributed to free CO in the glass, while the remaining photoproduct spectral features are attributed to coordinatively unsaturated $Os_3(CO)_{11}$ with an axial vacancy. (c) IR and UV–vis (inset) spectral changes and (d) associated IR difference spectrum obtained at 90 K for the glass photolyzed at 90 K (spectrum a), warmed to ~110 K, and recooled to 90 K again. The negative absorbance changes are associated with consumption of $Os_3(CO)_{12}$ during the initial photolysis; the positive absorbance changes are attributed to $Os_3(CO)_{11}(N_2)$, obtained by reaction of photogenerated $Os_3(CO)_{11}$ with excess N_2. Note the key feature at 2237 cm^{-1} assigned as the stretching frequency of coordinated N_2.

parison, Table I, of the spectral features for $Os_3(CO)_{11}(C_2H_4)$ and $Os_3(CO)_{11}(N_2)$ (vide infra), for which equatorial and axial ligand set geometries are, respectively, proposed. The IR spectral features for $Os_3(CO)_{11}$ are very similar to those observed for axially substituted complexes and are clearly indistinguishable from those observed for equatorially substituted complexes. In addition to this spectroscopic evidence, the accumulation of only the axially enriched isomer of $Os_3(CO)_{11}(^{13}CO)$ in the low-temperature reaction of photogenerated $Os_3(CO)_{11}$ with ^{13}CO (vide infra) serves to support description of the observed $Os_3(CO)_{11}$ photoproduct as structurally related to $Os_3(CO)_{12}$ by net creation of an axial vacancy.

The first electronic absorption feature for the $Os_3(CO)_{11}$ (524 nm) is much lower in energy and intensity than that for $Os_3(CO)_{12}$ (381 nm). The lower energy, weak absorption is consistent with significant stabilization of a localized d_z^2 level[38] that becomes the LUMO, in much the same way that coordinatively unsaturated mononuclear compounds are viewed,[2,3b] e.g., $Cr(CO)_5$ compared to $Cr(CO)_6$. Electronic spectral changes for the conversion of $Os_3(CO)_{12}$ to $Os_3(CO)_{11}$ are similar to those for thermal or photochemical conversion of $H_2Os_3(CO)_{11}$[49] to the coordinatively unsaturated $H_2Os_3(CO)_{10}$ complex[31] (vide infra). In particular, the purple $H_2Os_3(CO)_{10}$ complex exhibits a weak, low-energy feature which is absent in the yellow, coordinatively saturated $H_2Os_3(CO)_{11}$ complex, Table I. Furthermore, the first intense electronic transitions for axially vacant $Os_3(CO)_{11}$ and for $H_2Os_3(CO)_{10}$ are significantly blue-shifted compared to $Os_3(CO)_{12}$ and $H_2Os_3(CO)_{11}$, respectively. The electronic origin of the absorptions for $H_2Os_3(CO)_{10}$, however, is not straightforward owing to unsaturation delocalized by a four-center, $4e^-$ H_2Os_2 system.

(iii) Reactions of $Os_3(CO)_{11}$ with $2e^-$ Donor Ligands at Low Temperature. Direct kinetic control of the bimolecular reactions of photogenerated $Os_3(CO)_{11}$ with diffusing reagents is achieved at low temperature by proper choice of the glassing solvent, entering group concentration, and temperature. For 90 K alkane glasses containing photogenerated $Os_3(CO)_{11}$, photoejected CO, and an excess of either N_2, CO, or C_2H_4, thermal reaction according to eq 3 proceeds so rapidly in MP that the intermediacy

$$Os_3(CO)_{11} + L \xrightarrow[L = CO,\ C_2H_4,\ N_2]{\text{alkane, 110 K}} Os_3(CO)_{11}L \qquad (3)$$

of $Os_3(CO)_{11}$ is only established by rapid scan FTIR detection subsequent to a "flash photolysis" of the glass. Spectral features associated with photogenerated $Os_3(CO)_{11}$ decline with a half life of ~2–4 min in the presence of 3–5 mM CO or N_2 and with a half-life of 30 s in the presence of 50 mM C_2H_4. However, photogenerated $Os_3(CO)_{11}$ persists for hours in similarly prepared 90 K MCH glasses containing <5 mM CO, N_2, or C_2H_4. While a role for specific solvent interaction with photogenerated $Os_3(CO)_{11}$ may be important in the harder MCH glass, reaction of photogenerated $Os_3(CO)_{11}$ with ~3 mM H_2 in a MCH glass at 90 K (vide infra) suggests an alternative explanation. The N_2, CO, and C_2H_4 reagents are of essentially equal mass and are thus expected to have similar rates of diffusion that are far greater than the diffusion rate of the massive $Os_3(CO)_{11}$. A decreased diffusion rate for these ligands in MCH vs. MP likely contributes to the

medium effect observed at 90 K in the thermal reactions according to eq 3. Dihydrogen is a considerably more mobile entering group and diffuses freely in the 90 K MCH glass.

Reactions according to eq 3 only occur upon warming the MCH glasses to 110 K. Warmup to 110 K of a 90 K MCH glass containing photogenerated $Os_3(CO)_{11}$ and excess CO yields IR spectral changes consistent with quantitative regeneration of $Os_3(CO)_{12}$. In the absence of excess CO, $Os_3(CO)_{11}$ persists on warmup to 110 K, and no intermediates are detected during the course of further warmup necessary to quantitatively regenerate $Os_3(CO)_{12}$ by reaction with the CO present from the photogeneration of $Os_3(CO)_{11}$. After warmup to 110 K in the presence of excess CO, N_2, or C_2H_4, recooling the MCH glasses to 90 K permits acquisition of solvent corrected FTIR and UV–vis spectral changes associated with the net conversion of photogenerated $Os_3(CO)_{11}$ to product.

Warmup to 110 K of the 90 K MCH glass containing photogenerated $Os_3(CO)_{11}$ and excess N_2 (Figure 1 (parts a and b)) leads to rapid IR and UV–vis spectral changes which persist on recooling to 90 K (Figure 1 (parts c and d)). Figure 1c shows solvent corrected spectral features for a 90 K glass (1) prior to irradiation (as in Figure 1a) and (2) subsequent to the 110 K excursion. Figure 1d shows and IR difference spectrum associated with the net spectral changes presented in Figure 1c; the negative deviations correspond to consumption of $Os_3(CO)_{12}$ in the initial 90 K irradiation, while positive deviations indicate growth of spectral features associated with the product of reaction of photogenerated $Os_3(CO)_{11}$ with N_2. In Figure 1, the 110 K excursion leads to complete decline of the 524-nm and 2060-cm^{-1} features associated with the photogenerated $Os_3(CO)_{11}$, growth of a weak feature at 2237 cm^{-1} (Figure 1d, inset) associated with coordinated N_2, and growth of new IR spectral features in the region where $Os_3(CO)_{12}$ and $Os_3(CO)_{11}$ absorb. The 2237-cm^{-1} feature is too high in energy to be attributed to a CO stretching frequency and is clearly absent (Figure 1b, inset) prior to reaction of photogenerated $Os_3(CO)_{11}$ with N_2. The Raman active stretching vibrational frequency for N_2 in the gas phase[53] is 2331 cm^{-1}, and physical adsorption on a variety of substrates does little to alter this frequency.[54] The presence of N_2 as a ligand is therefore confirmed by the high wavenumber shift ($\Delta\nu = -94$ cm^{-1}) from the gas-phase value for N_2. A frequency measurement alone is not sufficient to distinguish between an end-on or a side-bound N_2 ligand. We note that the amount of photoejected CO (Figure 1b, inset) remains constant in the glass upon conversion of photogenerated $Os_3(CO)_{11}$ to the N_2-containing product (Figure 1d, inset). This result demonstrates that the N_2-containing product retains eleven CO's; net spectral changes in Figure 1d are consistent with the presence of one free CO (2132 cm^{-1}) for every $Os_3(CO)_{12}$ (2035 cm^{-1}) consumed in the initial photolysis. The IR spectral features for $Os_3(CO)_{11}(N_2)$ are closely related to those for $Os_3(CO)_{11}$ (Figure 1 (parts a and b)) and also to those observed for the axially substituted $Os_3(CO)_{11}L$ (L = $2e^-$) complexes. The conspicuous absence of any new low-energy electronic absorption features upon reaction of $Os_3(CO)_{11}$ and N_2 suggests that a coordinatively unsaturated product does not form. Restoration of electronic absorption spectral features to near coincidence with those for $Os_3(CO)_{12}$ (Figure 1c, inset) suggests retention of an unaltered metal–metal bonding framework in $Os_3(CO)_{11}(N_2)$ compared to that in $Os_3(CO)_{12}$. The spectral changes clearly suggest axial substitution of N_2 for CO on $Os_3(CO)_{12}$. Isotopic labelling experiments using $^{15}N_2$ confirm assignment of the high-energy vibrational feature for spectroscopically related $Ru_3(CO)_{11}(N_2)$ as the coordinated N_2 stretch.[19] On the basis of IR evidence we propose reaction of photogenerated $Os_3(CO)_{11}$ with N_2 according to eq 3. Warmup to 195 K of a 90 K alkane glass containing $Os_3(CO)_{11}(N_2)$, photoejected CO, and excess N_2 leads to quantitative regeneration of $Os_3(CO)_{12}$. Similarly, warmup to 298 K in the presence of 2 mM PPh_3 quantitatively yields $Os_3(CO)_{11}(PPh_3)$, consistent with our formulation of $Os_3(CO)_{11}(N_2)$. The N_2 adduct is clearly thermally labile with respect to substitution of N_2.

Warmup to 110 K of a 90 K MCH glass containing photogenerated $Os_3(CO)_{11}$ and excess C_2H_4 yields IR spectral changes which persist on recooling to 90 K, consistent with formation of one $Os_3(CO)_{11}(C_2H_4)$ molecule for each $Os_3(CO)_{12}$ molecule consumed in the initial irradiation. The identity of $Os_3(CO)_{11}(C_2H_4)$ was determined by comparison to spectral features obtained at 90 K for an authentic sample of $Os_3(CO)_{11}(C_2H_4)$. The equatorially substituted ligand set geometry for $Os_3(CO)_{11}(C_2H_4)$ has previously been established at 298 K by ^{13}C NMR spectroscopy,[43] consistent with the ligand set geometry found for structurally characterized $Os_3(CO)_{11}(CF_3(H)CC(H)CF_3)$[51] in the solid state. IR spectral data indicate that C_2H_4 occupies an equatorial substitution position at 90 K. The $Os_3(CO)_{11}(N_2)$ and $Os_3(CO)_{11}(C_2H_4)$ product molecules obtained from low-temperature reaction of photogenerated $Os_3(CO)_{11}$ with N_2 or C_2H_4 clearly exhibit IR spectral features consistent with axial and equatorial N_2 and C_2H_4, respectively. These results suggest a low thermal barrier to formation of the thermodynamically favored isomer of $Os_3(CO)_{11}L$ (L = N_2 and C_2H_4) upon low-temperature reaction according to eq 3.

(iv) Preparation of Axial-^{13}CO–$Os_3(CO)_{11}(^{13}CO)$. Photogenerated Os_3CO_{11} reacts with ^{13}CO in a kinetically controlled fashion to yield axial-^{13}CO–$Os_3(CO)_{11}(^{13}CO)$ under conditions where fluxional processes associated with interconversion of the two isoenergetic $Os_3(CO)_{11}(^{13}CO)$ isomers are completely suppressed. The photochemical loss of an equatorial CO from $Os_3(CO)_{12}$ can be established at low temperature by photolysis of axial-^{13}CO–$Os_3(CO)_{11}(^{13}CO)$ to yield a nonstatistical excess of photoejected ^{12}CO. First, the preparation of the axial-^{13}CO–$Os_3(CO)_{11}(^{13}CO)$ will be described.

Near-UV irradiation of ~0.1 mM $Os_3(CO)_{12}$ in a ^{13}CO-containing [99% ^{13}C, <4% ^{18}O; ~1 mM as judged by FTIR at $\nu(^{13}CO)$ = 2085 cm^{-1} (~400 M^{-1} cm^{-1} assuming $\epsilon(^{13}CO) \approx \epsilon(^{12}CO)$)[55]] MCH glass at 90 K yields IR (Figure 2a) and UV–vis spectral changes consistent with clean photogeneration of $Os_3(CO)_{11}$ and free ^{12}CO (2132 cm^{-1}) according to eq 1. Warmup of this irradiated 90 K glass to 110 K results in rapid IR spectral changes which persist on recooling to 90 K and which accompany complete restoration of all UV–vis spectral features to coincidence with those initially present for $Os_3(CO)_{12}$. Complete regeneration of $Os_3(CO)_{12}$ accompanies similar warmup in the presence of ~1 mM ^{12}CO, while photogenerated $Os_3(CO)_{11}$ persists undiminished in the absence of excess CO. Additional experiments establish that the absorbance decline at 2085 cm^{-1} (^{13}CO consumed) in the 110 K excursion is equal to the invariant absorbance at 2132 cm^{-1} (photoejected ^{12}CO). Figure 2b shows IR difference spectral changes at 90 K associated only with the 110 K excursion; the negative deviations (particularly the well-resolved feature at 2051 cm^{-1}) indicate complete consumption of photogenerated $Os_3(CO)_{11}$, while positive deviations are attributed to quantitative formation of $Os_3(CO)_{11}(^{13}CO)$.

After forming $Os_3(CO)_{11}(^{13}CO)$ at low temperature, Figure 2, warmup to 300 K of the 90 K MCH glass yields new IR spectral changes which persist on recooling to 90 K, Figure 3, consistent with conversion of the low-temperature product to a mixture of isomers of $Os_3(CO)_{11}(^{13}CO)$. Figure 3a shows a comparison of IR difference spectra obtained for the irradiated glass at 90 K after the initial 110 K excursion (reproduced from Figure 2b) and after the subsequent 300 K excursion. Coincidence of the negative deviations at 2051 cm^{-1} for the two traces confirms complete consumption of photogenerated $Os_3(CO)_{11}$ in the initial 110 K

(52) Benfield, R. E.; Johnson, B. F. G.; Raithby, P. R.; Sheldrick, G. M. *Acta Crystallogr., Sect. B: Struct. Crystallogr. Cryst. Chem.* **1978**, *B34*, 666–667.

(53) Szymanski, H. S. *Raman Spectroscopy*, Plenum Press: New York/London, 1970; Vol. 2.

(54) Wang, H. P.; Yates, J. T., Jr. *J. Phys. Chem.* **1984**, *88*, 852–856.

(55) Near-UV irradiation of $Os_3(CO)_{12}$ in a ^{13}CO-saturated MP glass at 90 K yields, after equilibration, substitutions of ^{12}CO by ^{13}CO without net change in the UV–vis spectral features associated with the trinuclear metal framework. The final absorbance changes at 2132 cm^{-1} (^{12}CO) and 2085 cm^{-1} (^{13}CO) are of equal magnitude, suggesting that the extinction coefficients for ^{12}CO and ^{13}CO differ by less than 5% in MP at 90 K ($^{13}C^{18}O$ content is <4%).

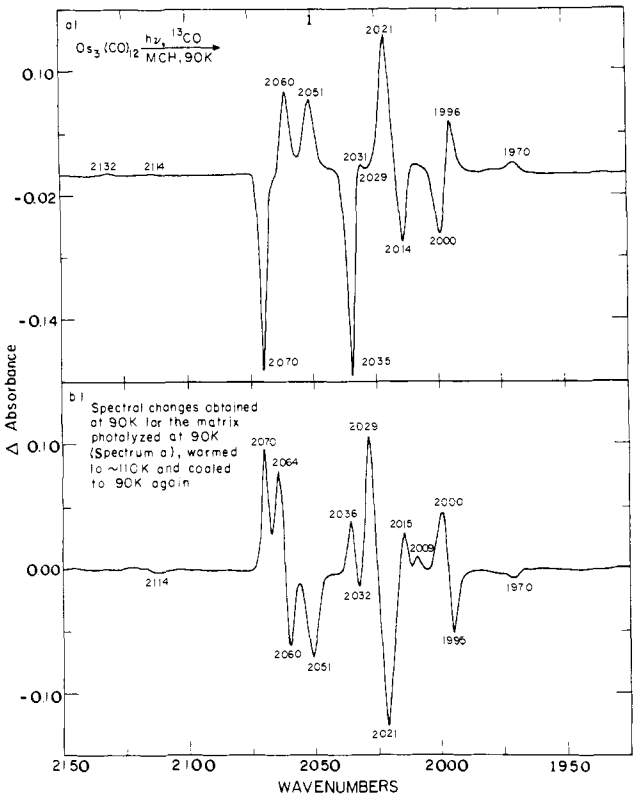

Figure 2. (a) IR difference spectral changes accompanying near-UV irradiation of 0.1 mM $Os_3(CO)_{12}$ in a 90 K MCH glass containing ~1.0 mM ^{13}CO. The band at 2132 cm^{-1} is attributed to free ^{12}CO in the glass; remaining photoproduct spectral features are attributed to photogenerated $Os_3(CO)_{11}$. (b) IR difference spectral changes at 90 K associated with warming the irradiated glass (spectrum a) to ~110 K and recooling it to 90 K. Negative deviations indicate consumption of photogenerated $Os_3CO)_{11}$; positive deviations are attributed to formation of axial-^{13}CO–$Os_3(CO)_{11}(^{13}CO)$.

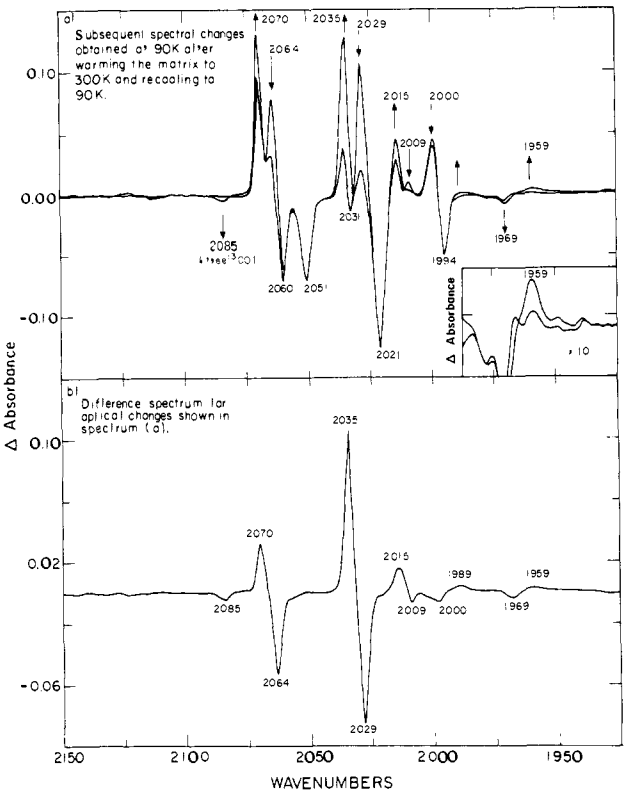

Figure 3. (a) IR difference spectra obtained at 90 K for the irradiated, annealed glass of Figure 2 before and after warming it to 300 K and recooling it to 90 K again. For both traces, negative deviations are associated with consumption of photogenerated $Os_3(CO)_{11}$ during the initial 110 K excursion (Figure 2); the positive deviations are associated with axial-^{13}CO–$Os_3(CO)_{11}(^{13}CO)$ after the initial 110 K excursion (trace redrawn from Figure 2b) or an equilibrium mixture (1:1) of axial- and equatorial-^{13}CO–$Os_3(CO)_{11}(^{13}CO)$ after the 300 K excursion. (b) IR difference spectral changes at 90 K associated only with the 300 K excursion (difference between the two traces in spectrum (a)). The declining 2085 cm^{-1} feature is associated with loss of excess ^{13}CO from the solution during warmup to 300 K; remaining negative deviations are associated with partial decline of axial-^{13}CO–$Os_3(CO)_{11}(^{13}CO)$; positive deviations are attributed to formation of equatorial-^{13}CO–$Os_3(CO)_{11}(^{13}CO)$.

excursion. The positive deviations associated with $Os_3(CO)_{11}(^{13}CO)$ clearly change as a result of the 300 K excursion; net changes associated only with the 300 K excursion are presented as a difference IR spectrum in Figure 3b. The $Os_3(CO)_{12}$, and presumably $Os_3(CO)_{11}(^{13}CO)$, complexes are thermally inert under the conditions of this experiment[56] as confirmed by observation that the 90 K UV–vis spectral features remain unaffected by the 300 K excursion. The final IR spectral features for $Os_3(CO)_{11}(^{13}CO)$ are in close agreement with those reported previously[39] for $Os_3(CO)_{11}(^{13}CO)$ in alkane media at 300 K. The IR spectral changes associated with the 300 K excursion, Figure 3, are therefore most consistent with equilibration of the two isoenergetic isomers (axial and equatorial ^{13}CO) of $Os_3(CO)_{11}(^{13}CO)$ following initial formation, in the 110 K excursion, of a nonstatistical excess of one isomer of $Os_3(CO)_{11}(^{13}CO)$ as the low-temperature product of reaction of photogenerated $Os_3(CO)_{11}$ with ^{13}CO. Previous ^{13}C NMR investigations[57] for $Os_3(CO)_{12}$ indicate that complete equilibration of the $Os_3(CO)_{11}(^{13}CO)$ isomers should be rapid on the time scale of the 300 K excursion. Notably, no further IR spectral changes accompany a second excursion to 300 K. The negative deviations in Figure 3b are therefore attributed to decline of spectral features associated with the isomer initially in excess, while positive deviations are associated with conversion to the second isomer.

Equal amounts of the two isoenergetic $Os_3(CO)_{11}(^{13}CO)$ isomers are expected to obtain at equilibrium. The 90 K IR spectral changes associated with the 300 K excursion in Figure 3 are consistent with a full 50% (±5%) decline in the intense 2029- and weak 1969-cm^{-1} product features associated with the $Os_3(CO)_{11}(^{13}CO)$ isomer initially in excess (this result obtains after correction for declining $Os_3(CO)_{11}$ spectral features in Figure 3a). The extent of this absorbance decline is consistent with the conclusion that the 2029- and 1969-cm^{-1} features are uniquely attributable to one isomer of $Os_3(CO)_{11}(^{13}CO)$, initially present as the only product of low-temperature reaction of photogenerated $Os_3(CO)_{11}$ with ^{13}CO. A smaller absorbance decline (or even an increase) is expected at frequencies where both isomers absorb. The growth of a weak IR spectral feature at 1959 cm^{-1} (Figure 3a, inset), well-resolved from initial product absorptions, is therefore uniquely attributable to the second isomer of $Os_3(CO)_{11}(^{13}CO)$. The IR spectral features for each of the two $Os_3(CO)_{11}(^{13}CO)$ isomers have been deconvoluted, Table I. The low-temperature product has been assigned as the $Os_3(CO)_{11}(^{13}CO)$ isomer with ^{13}CO in an axial position on the basis of the following considerations.

Solid-state Raman spectroscopy[39] has yielded results insufficient to unambiguously differentiate between an axially dominant $\nu_5(e')$ or a pure axial $\nu_4(a_2'')$ assignment[58] for the highest energy, IR active feature for $Os_3(CO)_{12}$ at 2070 cm^{-1}. The 2064- and 2070-cm^{-1} (or 2065- and 2070-cm^{-1}) features associated with the initial (or second) isomer of $Os_3(CO)_{11}(^{13}CO)$ have the same molecular origin as the 2070-cm^{-1} feature for $Os_3(CO)_{12}$, consistent

(56) Shojaie, A.; Atwood, J. D. *Organometallics* **1985**, *4*, 187–190.
(57) (a) Aime, S.; Gambino, O.; Milone, L.; Sappa, E.; Rosenberg, E. *Inorg. Chim. Acta* **1975**, *15*, 53–56. (b) Forster, A.; Johnson, B. F. G.; Lewis, J.; Matheson, T. W.; Robinson, B. H.; Jackson, W. G. *J. Chem. Soc., Chem. Commun.* **1974**, 1042–1044.

(58) Here "axial" and "radial" (equatorial) refer to the symmetry coordinate which dominates in the vibration.

Scheme I. Reaction of Photogenerated $Os_3(CO)_{11}$ with ^{13}CO

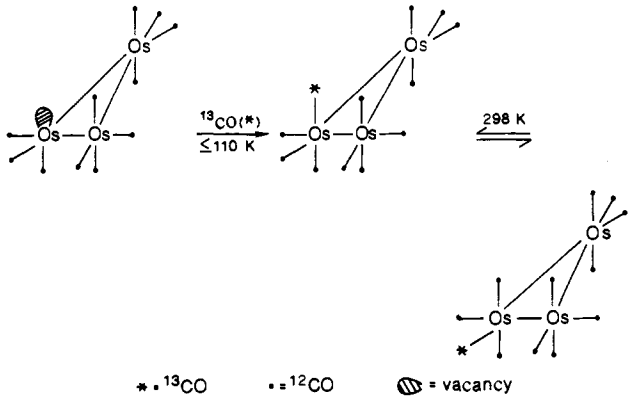

with splitting of degeneracy associated only with the $\nu_5(e')$ assignment in $Os_3(CO)_{12}$. After assignment of the highest energy IR band to an e' mode, there is no other reasonable candidate for the $\nu_4(a_2'')$ mode[39,59,60] than the intense 2035-cm^{-1} feature for $Os_3(CO)_{12}$. The correlation of this purely axial mode through the $Os_3(CO)_{11}(^{13}CO)$ isomers is quite unambiguous, with intense features appearing at 2029 cm^{-1} for the low-temperature product and at 2035 cm^{-1} for the second isomer. These relative energies are only compatible with assignment to axial- and equatorial-^{13}CO–$Os_3(CO)_{11}(^{13}CO)$, respectively, Table I. Consistent with this assignment we note that the axial-to-equatorial isomerization of $Os_3(CO)_{11}(^{13}CO)$ leads to intensity changes at 2070 and 2064 cm^{-1} (Figure 3b) which can be related to a dominant contribution of axial CO oscillators to the parent e' mode of $Os_3(CO)_{12}$.[39] The low-temperature accumulation of axial-^{13}CO–$Os_3(CO)_{11}(^{13}CO)$ is consistent with the IR spectral characterization of the photogenerated $Os_3(CO)_{11}$ precursor as an axially vacant fragment, Scheme I.

The equilibrated mixture of $Os_3(CO)_{11}(^{13}CO)$ isomers has been previously characterized by IR spectroscopy in alkane media at 298 K, and vibrational assignments have been proposed by Battiston et al.[39] as part of a detailed vibrational analysis of $M_3(CO)_{12}$ (M = Os, Ru) complexes. The predicted contributions of individual isomers to this spectrum are in excellent agreement with our experimental results, Table I. The force constant calculations of Battiston et al.[39] for $M_3(CO)_{12}$ (M = Os, Ru) complexes were hampered by uncertainty in $\nu_2(a_1')$, $\nu_3(a_2')$, and $\nu_8(e'')$, which were optimized under the constraints of available isotopic frequencies and a "good" set of resulting force and interaction constants. The weak 2036-cm^{-1} feature for axial-^{13}CO–$Os_3(CO)_{11}(^{13}CO)$ can have no other origin than, and enables direct calculation of, the $\nu_2(a_1')$ mode for $Os_3(CO)_{12}$. This feature was unobservable by Battiston et al.[39] for a mixture of $Os_3(CO)_{11}(^{13}CO)$ isomers due to overlap by the intense 2035-cm^{-1} feature associated with equatorial-^{13}CO–$Os_3(CO)_{11}(^{13}CO)$. Proper correlation of the $\nu_8(e'')$ and $\nu_3(a_2')$ modes of $Os_3(CO)_{12}$ with the two low-energy isotopic satellites which derive mainly from them is experimentally determined by our correlation of these satellites with individual isomers of $Os_3(CO)_{11}(^{13}CO)$. The $\nu_3(a_2')$ mode is a purely radial mode[58] and is therefore related to the low-energy satellite for equatorial-^{13}CO–$Os_3(CO)_{11}(^{13}CO)$ (found at 1959 cm^{-1}). The $\nu_8(e'')$ mode is purely axial and is therefore related to the low-energy satellite for axial-^{13}CO–$Os_3(CO)_{11}(^{13}CO)$ (found at 1969 cm^{-1}). These satellites clearly indicate the presence of two all-^{12}CO frequencies in the region between 2000 and 1990 cm^{-1} where only the $\nu_3(a_2')$ and $\nu_8(e'')$ modes are realistic candidates.[39,59,60] Our results strongly support the findings of the theoretical investigation of Battiston et al.[39]

(v) Photodissociative Loss of Equatorial ^{12}CO from Axial-^{13}CO–$Os_3(CO)_{11}(^{13}CO)$ at 90 K. Near-UV irradiation of a 90 K MCH glass containing axial-^{13}CO–$Os_3(CO)_{11}(^{13}CO)$, unreacted

Scheme II. Proposed Stereochemistry for Light-Induced Dissociative Loss of CO from $Os_3(CO)_{12}$ at 90 K

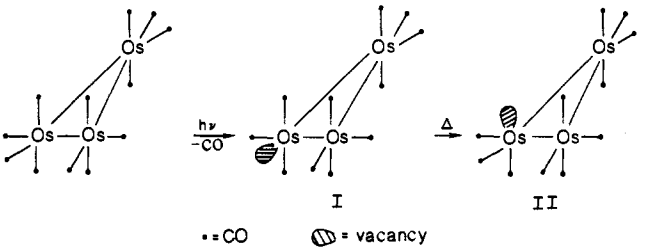

$Os_3(CO)_{12}$ (<10%), photoejected CO, and excess ^{13}CO leads to clean UV–vis spectral changes indistinguishable from those obtained in the photoconversion of $Os_3(CO)_{12}$ to coordinatively unsaturated $Os_3(CO)_{11}$. Associated IR spectral changes are very complicated in the region where $Os_3(CO)_{11}(^{13}CO)$ absorbs. The key result is that *no* absorbance change is detected at 2085 cm^{-1} (^{13}CO), whereas significant growth of absorbance occurs at 2132 cm^{-1} (^{12}CO). Our results place a lower limit of 28 on the ratio of photoejected $^{12}CO/^{13}CO$ in this photoconversion. ^{13}CO is detected ($^{12}CO/^{13}CO \approx 10$–$14$) when an equilibrated mixture of axial- and equatorial-^{13}CO–$Os_3(CO)_{11}(^{13}CO)$ is irradiated at 90 K. Our results suggest selective photodissociation of equatorial CO from axial-^{13}CO–$Os_3(CO)_{11}(^{13}CO)$ and therefore photogeneration of $Os_3(CO)_{11}$ from $Os_3(CO)_{12}$ according to Scheme II. While the accurate determination of small absorbance changes at 2085 cm^{-1} might be complicated by the temperature sensitive absorbance associated with ^{13}CO initially in excess, the reproducible absence of any such absorbance change upon irradiation of axial-^{13}CO–$Os_3(CO)_{11}(^{13}CO)$ in these glasses is consistent with our expectation (vide infra) that the third electronic absorption, responsible for CO loss, labilizes the equatorial CO's of $Os_3(CO)_{12}$. Recombination of geminate free CO with equatorially vacant $Os_3(CO)_{11}$ (I) may be inhibited by isomerization to axially vacant $Os_3(CO)_{11}$ (II).[61,62] The wavelength dependent accumulation of II would then simply reflect an increase in the kinetic energy for photoejected CO or, alternatively, an increase in the efficiency for isomerization of $Os_3(CO)_{11}$ at higher excitation energies. We do not favor these mechanisms because only one type of uncomplexed CO is observed by IR following photosubstitution. Furthermore, the corresponding wavelength-dependent photosubstitution quantum yields in fluid solution at 298 K are not readily explained by such mechanisms. We believe that the wavelength dependence is due to differences in reactivity associated with different electronic states.

(vi) The Nature of the Excited State Responsible for Photodissociative Loss of CO from $Os_3(CO)_{12}$. The wavelength dependence for loss of equatorial CO can be understood by consideration of the electronic structure of $Os_3(CO)_{12}$. Frontier orbital splittings obtained by Trogler and co-workers[38] in a multipolar potential discrete variational X_α calcualtion for $M_3(CO)_{12}$ (M = Os, Ru) correctly predict a small a_1'–e' orbital splitting and a large d-band splitting as established by photoelectron spectroscopy.[38,63] For both $Ru_3(CO)_{12}$ and $Os_3(CO)_{12}$, the dipole-forbidden $10a_1' \rightarrow 6a_2'$ ($^1A_1' \rightarrow {}^1A_2'$) transition is calculated to be lowest in energy, closely followed by the allowed electronic transitions $15e' \rightarrow 6a_2'$ ($^1A_1' \rightarrow {}^1E'$) and $10a_1' \rightarrow 16e'$ ($^1A_1' \rightarrow {}^1E'$). Spectroscopic studies[40] for $Ru_3(CO)_{12}$ and $Os_3(CO)_{12}$ have suggested, however, that the $10a_1' \rightarrow 16e'$ transition in $Os_3(CO)_{12}$ is lower in energy

(59) Quicksall, C. O.; Spiro, T. G. *Inorg. Chem.* **1968**, *7*, 2365–2369.
(60) Huggins, D. K.; Flitcroft, N.; Kaesz, H. D. *Inorg. Chem.* **1965**, *4*, 166–169.

(61) Isomerization has been invoked to explain photoreversible CO loss from $Cr(CO)_6$ in a noble gas matrix at 20 K: (a) Burdett, J. K.; Perutz, R. N.; Poliakoff, M.; Turner, J. J. *J. Chem. Soc., Chem. Commun.* **1975**, 157–159. (b) Burdett, J. K.; Grzybowski, J. M.; Perutz, R. N.; Poliakoff, M.; Turner, J. J.; Turner, R. F. *Inorg. Chem.* **1978**, *17*, 147–154.
(62) Isomerization from a vibrationally hot ground state has precedence in the infrared laser induced isomerization of $Fe(CO)_4$ in Ar matrices at 20 K: Davies, B.; McNeish, A.; Poliakoff, M.; Turner, J. J. *J. Am. Chem. Soc.* **1977**, *99*, 7573–7579.
(63) (a) Ajo, D.; Granozzi, G.; Tondello, E.; Fragala, I. *Inorg. Chim. Acta* **1979**, *37*, 191–193. (b) Green, J. C.; Seddon, E. A.; Mingos, D. M. P. *J. Chem. Soc., Chem. Commun. 1979*, 94–95. Green, J. C.; Seddon, E. A.; Mingos, D. M. P. *Inorg. Chem.* **1981**, *20*, 2595–2602.

than the $15e' \rightarrow 6a_2'$ transition. The $14e' \rightarrow 6a_2'$ ($^1A_1' \rightarrow {}^1E'$) transition is calculated to be at higher energy. The third allowed electronic transition ($14e' \rightarrow 6a_2'$), responsible for the dissociative loss of CO from $Os_3(CO)_{12}$, approximates a $\sigma^{*\prime} \rightarrow \sigma^*$ transition from an orbital of predominantly $d_{x^2-y^2}$ character (directed between the equatorial CO ligands and toward the center of the triangular metal–metal framework) to an orbital of predominantly d_{xy}, p_x, and p_y character (directed toward the equatorial CO ligands and along the edges of the triangular metal–metal framework). This redistribution of electron density within the plane defined by the trinuclear metal framework is therefore expected to greatly destabilize equatorial M–CO bonding without affecting the net metal–metal bond order for the cluster. Dissociative loss of only ^{12}CO from axial-^{13}CO–$Os_3(CO)_{11}(^{13}CO)$ in a 90 K MCH glass is in accord with this expectation. The 298 K photosubstitution efficiencies increase dramatically with irradiation energy consistent with the increasing contribution of the third electronic absorption. The wavelength dependence of the 298 K photosubstitution efficiencies[13] and the 90 K CO loss efficiencies[19] for $Ru_3(CO)_{12}$ in alkane media are quite similar to those reported here for $Os_3(CO)_{12}$. Obviously, one cannot rule out labilization of CO from a vibrationally nonequilibrated electronic state(s) to yield more efficient photodissociation at higher excitation energies.

(vii) Oxidative Addition of H_2 to Photogenerated $Os_3(CO)_{11}$. Near-UV irradiation of $Os_3(CO)_{12}$ in H_2-saturated alkane solution proceeds at 298 K according to eq 4 with a 366-nm quantum yield

$$Os_3(CO)_{12} \xrightarrow[\text{alkane, 298 K}]{h\nu,\ H_2} H_2Os_3(CO)_{10} + 2CO \qquad (4)$$

of 0.02 ± 0.005, indistinguishable from that obtained for photosubstitution of CO by PPh_3. In accord with preliminary findings,[7] we have developed a high yield photochemical synthesis of $H_2Os_3(CO)_{10}$ based on this chemistry (see Experimental Section). The intermediacy of $H_2Os_3(CO)_{11}$, eq 5 and 6, in the photoconversion presented in eq 4 is established at 298 K by FTIR detection subsequent to a "flash photolysis" (50 μs) irradiation of $Os_3(CO)_{12}$ (0.2 mM) in H_2-saturated isooctane solution. The initial IR spectral changes (within 10 s of the flash) are consistent with ~10% consumption of $Os_3(CO)_{12}$ (2069 cm^{-1}) to yield primarily $H_2Os_3(CO)_{11}$ (~80%, 2088 cm^{-1}) and some $H_2Os_3(CO)_{10}$ (~20%, 2075 cm^{-1}), Table I. Consistent with the known thermal lability of $H_2Os_3(CO)_{11}$,[31] eq 6, this product distribution changes to ~10% $H_2Os_3(CO)_{11}$ and ~90% $H_2Os_3(CO)_{10}$ after 4 h in the dark at 298 K. Efficient photochemical acceleration of this conversion according to eq 6 (Φ_{366} = 0.2 in alkane at 298 K)[64] prevents accumulation of $H_2Os_3(CO)_{11}$ during continuous near-UV irradiation of $Os_3(CO)_{12}$ in the presence of H_2. Interestingly, near-UV irradiation of an independently prepared sample of $H_2Os_3(CO)_{11}$ in MP at 90 K quantitatively yields $H_2Os_3(CO)_{10}$ and free CO. The conspicuous absence of $Os_3(CO)_{11}$ as a photoproduct shows that reductive elimination of H_2 is not competitive with CO loss from $H_2Os_3(CO)_{11}$ at 90 K.

$$Os_3(CO)_{12} + H_2 \xrightarrow{h\nu} H_2Os_3(CO)_{11} + CO \qquad (5)$$

$$H_2Os_3(CO)_{11} \xrightarrow[\text{alkane}]{\Delta \text{ or } h\nu} H_2Os_3(CO)_{10} + CO \qquad (6)$$

The intermediacy of photogenerated $Os_3(CO)_{11}$ in the net photochemical conversion of $Os_3(CO)_{12}$ to $H_2Os_3(CO)_{10}$ can be demonstrated at low temperature in an H_2-containing MCH glass. Near-UV irradiation of $Os_3(CO)_{12}$ (0.1 mM) in a 90 K MCH glass, originally handled in a H_2-containing Ar atmosphere, yields IR spectral changes (presented as Supplementary Material) associated with the clean photogeneration of $Os_3(CO)_{11}$ and free CO (2132 cm^{-1}). Warmup of this irradiated 90 K glass to 130 K results in IR spectral changes which persist on recooling to 90 K, consistent with conversion of irreversibly consumed $Os_3(CO)_{12}$ (2070 cm^{-1}) predominantly to $H_2Os_3(CO)_{11}$ (2088 cm^{-1}). Net IR spectral changes associated only with the 130 K excursion indicate that photogenerated $Os_3(CO)_{11}$ reacts with H_2 to form $H_2Os_3(CO)_{11}$, Scheme III, and with photoejected CO to regenerate significant amounts of $Os_3(CO)_{12}$. Similar 90 K irradiation of $Os_3(CO)_{12}$ in a MCH glass containing higher concentrations of H_2 yields $H_2Os_3(CO)_{10}$, $Os_3(CO)_{11}$, and minor amounts of $H_2Os_3(CO)_{11}$ (Supplementary Material). Subsequent thermal reaction of the photogenerated $Os_3(CO)_{11}$ with H_2 at 90 K yields quantitative formation of one $H_2Os_3(CO)_{11}$ for every $Os_3(CO)_{11}$ consumed, Scheme III. The $H_2Os_3(CO)_{11}$ complex, accumulated thermally in these glasses, undergoes photochemical conversion to $H_2Os_3(CO)_{10}$ and additional free CO on a time scale which is rapid with respect to disappearance of remaining $Os_3(CO)_{12}$ at 90 K.

Scheme III. Oxidative Addition of H_2 to Photogenerated $Os_3(CO)_{11}$

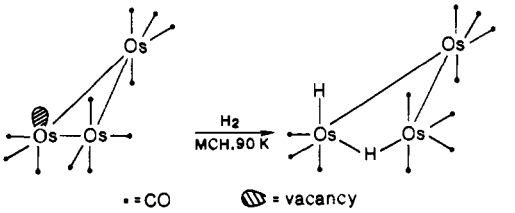

Our results establish oxidative addition of H_2 to photogenerated $Os_3(CO)_{11}$, having a localized axial vacancy. These results relate to a previous proposal that the *thermal* reaction of $Os_3(CO)_{12}$ with H_2 proceeds by CO loss, oxidative addition of H_2 to thermally generated $Os_3(CO)_{11}$ to form undetected $H_2Os_3(CO)_{11}$, and loss of a second CO to yield $H_2Os_3(CO)_{10}$ as the isolated coordinatively unsaturated product.[65]

(B) Long Wavelength Photochemistry of $Os_3(CO)_{12}$. (i) Associative Photosubstitution of $Os_3(CO)_{12}$ at 90 K. The following evidence supports associative substitution of strong π-acceptor ligands for CO during selective irradiation into the second electronic absorption for $Os_3(CO)_{12}$ at 90 K. Broad band (quartz-filtered) irradiation of $Os_3(CO)_{12}$ at 90 K in (a) a MCH glass, (b) an N_2-containing MP glass, (c) a 2-MeTHF glass, (d) a C_2H_4-saturated MP glass, or (e) a 1-pentene glass results in spectral changes showing the photoejection of one CO for every $Os_3(CO)_{12}$ consumed. New IR spectral features attributed to formation of $Os_3(CO)_{11}$ or $Os_3(CO)_{11}L$ (L = N_2, 2-MeTHF, C_2H_4, C_5H_{10}, respectively) complexes are found. Percent conversions vary linearly with irradiation time at low extents (<10%) of conversion. Percent conversions, normalized to 5 min of irradiation, are reported in Table IIb for each glass. The IR spectral features for $Os_3(CO)_{11}(C_5H_{10})$ are nearly the same as those reported previously[43] for $Os_3(CO)_{11}(C_2H_4)$. Warmup to 298 K of the irradiated 1-pentene or 2-MeTHF glasses quantitatively regenerates $Os_3(CO)_{12}$, while similar warmup in the presence of 2 mM PPh_3 quantitatively yields $Os_3(CO)_{11}(PPh_3)$. These results support our formulation of the $Os_3(CO)_{11}(C_5H_{10})$ and $Os_3(CO)_{11}$(2-MeTHF) complexes. The related $Os_3(CO)_{11}(C_2H_4)$[43] and $Os_3(CO)_{11}$(THF)[66] complexes, respectively, have both been reported to be substitution labile. Broad band photoreaction rates in all but one medium, 1-pentene, are the same. The photoreaction rate in 1-pentene is twice that in the other glasses. Selective excitation (λ > 370 nm) into the first electronic absorption of $Os_3(CO)_{12}$ yields negligible photochemistry in all of the glasses at 90 K in accord with the extremely inefficient photochemistry obtained for 436-nm irradiation of $Os_3(CO)_{12}$ in PPh_3-containing solutions at 298 K. Selective excitation into the second electronic absorption at 90 K with 313-nm irradiation yields net photochemistry only in glasses d and e to form an $Os_3(CO)_{11}(\eta^2$-alkene) complex and free CO (2132 cm^{-1}). Photosubstitution of ^{13}CO for ^{12}CO also obtains for 313-nm, but not λ > 370-nm, irradiation of $Os_3(CO)_{12}$ in a ^{13}CO-containing MP glass at 90 K. Pyrex-filtered (λ > 280-nm) irradiation yields relative photoconversion efficiencies, Table IIb, for photochemistry associated principally

(64) Graff, J. L. Ph.D. Thesis, M.I.T., 1981.

(65) Kaesz, H. D.; Knox, S. A. R.; Koepke, J. W.; Saillant, R. B. *J. Chem. Soc., Chem. Commun.* 1971, 477.

(66) Jensen, C. M.; Knobler, C. B.; Kaesz, H. D. *J. Am. Chem. Soc.* **1984**, *106*, 5926–5933.

with the second allowed electronic absorption of $Os_3(CO)_{12}$.

The two low-energy, allowed electronic transitions are apparently relatively unimportant in the photochemistry of $Os_3(CO)_{12}$ in MCH at 90 K; photogeneration of $Os_3(CO)_{11}$ only results upon higher energy excitation. The low-temperature photosubstitution of 2-MeTHF (c) or N_2 (b) for CO on $Os_3(CO)_{12}$ can be accounted for completely by the intermediacy of photogenerated $Os_3(CO)_{11}$, because the photoreaction efficiencies are the same in glasses a–c. The results in 2-MeTHF at 90 K are in keeping with the observation at 298 K that the photosubstitution quantum yields are unaffected by the added presence of 0.1 M THF. However, because there is a strong entering group effect on the photoreaction efficiency at 90 K, we suggest an associative substitution pathway is important in the presence of strong π-acids such as C_2H_4 (d), C_5H_{10} (e), and ^{13}CO upon excitation into the second electronic absorption.

The long wavelength photochemistry obtained for $Os_3(CO)_{12}$ at 90 K is consistent with reaction of strong π-acceptor ligands and a reactive isomer or excited state of $Os_3(CO)_{12}$ to give associative substitution via a $Os_3(CO)_{12}L$-type adduct. Thermodynamic and/or cage effects suppress fragmentation of this adduct in favor of competing ligand loss (CO or L) to yield the substitution product or to regenerate $Os_3(CO)_{12}$, respectively. The entering group dependence would reflect the notion that net reaction from the $Os_3(CO)_{12}L$ adduct is related to the π-back-bonding ability of L. Importantly, a $Os_3(CO)_{12}L$ intermediate may also be involved in the photofragmentation of $Os_3(CO)_{12}$ in PPh_3-, C_2H_4-, or CO-containing fluid solutions, where long wavelength photofragmentation is favored for strong π-acceptor ligands (C_2H_4 and CO, not PPh_3).

(ii) Photofragmentation of $Os_3(CO)_{12}$ in Fluid Solutions. For $\lambda > 370$-nm irradiation into the overlapping first and second allowed electronic transitions of $Os_3(CO)_{12}$ in PPh_3-saturated alkane solutions at 298 K, careful inspection of the FTIR spectral changes at 2% conversion reveals that $Os(CO)_4(PPh_3)$,[67] Table I, is also formed as a primary photoproduct in trace amounts. There is >98% conversion to $Os_3(CO)_{11}(PPh_3)$ as determined by FTIR. The $Os_3(CO)_{10}(PPh_3)_2$ complex[44] is never observed at low extent (~2%) conversion. At 195 K, $\lambda > 370$-nm irradiation initially generates <80% $Os_3(CO)_{11}(PPh_3)$, along with *significant* quantities of $Os(CO)_4(PPh_3)$ and minor amounts of $Os(CO)_3(PPh_3)_2$.

Prolonged near-UV irradiation of $Os_3(CO)_{12}$ in CO-saturated alkane solution at 298 K yields no FTIR spectral changes, in accord with a previous investigation in CH_3CN as solvent.[18] However, similar irradiation at 195 K slowly generates a mixture of $Os(CO)_5$ and $Os_2(CO)_9$, Table I; subsequent warmup of the irradiated 195 K solution to 298 K regenerates $Os_3(CO)_{12}$ in accord with the known thermal lability of the 195 K photoproducts.[68]

Interestingly, long wavelength excitation ($\lambda > 370$ nm) of $Os_3(CO)_{12}$ in olefin-containing solutions has previously been reported[10] to yield $Os(CO)_4(\eta^2$-olefin) and $Os_2(CO)_8(\mu$-η^1,η^1-CHRCHR′) derivatives. We find that $\lambda > 370$-nm irradiation of $Os_3(CO)_{12}$ in C_2H_4-saturated alkane media[46] at 298 K leads to IR spectral changes at low extent conversion consistent with initial formation of ~60% $Os_3(CO)_{11}(C_2H_4)$,[43] along with $Os(CO)_4(C_2H_4)$[69] and $Os_2(CO)_8(\mu$-η^1,η^1-$CH_2CH_2)$.[70] Only the latter two complexes accumulate and persist at longer irradiation times in accord with the previously reported isolation of only these two products[10] during preparative photoreactions. Curiously, we do not find the diosmacyclobutane upon $\lambda > 370$-nm irradiation at 195 K; the $Os_3(CO)_{11}(C_2H_4)$ and $Os(CO)_4(C_2H_4)$ complexes are observed as initial photoproducts at <2% conversion of $Os_3(CO)_{12}$, but the $Os_3(CO)_{11}(C_2H_4)$ never accumulates under these conditions. The $Os_3(CO)_{12}$ is quantitatively consumed to yield predominantly $Os(CO)_4(C_2H_4)$ and trace amounts of a species formulated as $Os(CO)_3(C_2H_4)_2$. Subsequent broad band irradiation of this solution at 195 K results in the decline of IR spectral features for $Os(CO)_4(C_2H_4)$, accompanied by initially increased yields of $Os(CO)_3(C_2H_4)_2$ and eventually *trans*-$Os(CO)_2(C_2H_4)_3$, both products being tentatively formulated based on FTIR spectral similarity to the analogous Fe and Ru systems.[71] Irradiation of $Os_3(CO)_{12}$ at 313 nm in C_2H_4-saturated alkane solution yields $Os_3(CO)_{11}(C_2H_4)$ as the only detected primary photoproduct at 195 or 298 K, consistent with the CO loss established for excitation into the third allowed electronic transition of $Os_3(CO)_{12}$.

(iii) Nature of the Excited State Responsible for Photofragmentation and Associative Photosubstitution of $Os_3(CO)_{12}$. The first ($10a_1' \rightarrow 16e'$) and second ($15e' \rightarrow 6a_2'$) allowed electronic absorptions for $Os_3(CO)_{12}$ are not well-resolved at 298 K, and the contributions of each to the observed photochemistry are not clearly established by our experiments at 298 K. Nevertheless, the long wavelength photofragmentation reported here and elsewhere[72] is most consistent with the nature of the $15e' \rightarrow 6a_2'$ transition. As noted previously,[40] the temperature dependent behavior observed here for the second electronic absorption for $Os_3(CO)_{12}$ (it sharpens and blue-shifts from 330 to 320 nm on cooling from 298 to 90 K) is quite similar to that observed for the lowest energy absorption of $Ru_3(CO)_{12}$, consistent with their common assignment to the $15e' \rightarrow 6a_2'$ ($^1A_1' \rightarrow {}^1E'$) transition. The 15e′ and $6a_2'$ orbitals contain significant d_{xy} and $p_{x,y}$ orbital character destabilized by direction toward the equatorial CO ligand. The two-filled edge-bonding 15e′ orbitals are responsible for most of the metal–metal bonding in $Os_3(CO)_{12}$.[38] Analyzed in terms of the properties of virtual orbitals for the ground state, the $15e' \rightarrow 6a_2'$ transition approximates a $\sigma \rightarrow \sigma^*$ transition for orbitals that overlap along the edges of the triangular metal framework. The associative photosubstitution behavior attributed to 90 K excitation into the second electronic absorption of $Os_3(CO)_{12}$ parallels the photochemistry associated with the first (lowest energy) absorption of $Ru_3(CO)_{12}$,[19] for which dissociative loss of CO is not important at 90 K and for which photofragmentation efficiencies at 298 K[13] and associative photosubstitution efficiencies at 90 K[19] are greater for strong π-acceptor ligands. Photofragmentation of $Os_3(CO)_{12}$ in fluid solution appears to be selective of the strong π-acid C_2H_4 (compared to PPh_3), suggesting the possible involvement of an intermediate related to that responsible for the photofragmentation of $Ru_3(CO)_{12}$.[13,17] For $\lambda > 370$-nm irradiation of $Os_3(CO)_{12}$ in PPh_3- or C_2H_4-containing solutions, the ratio of photosubstitution to photofragmentation products is less at 195 K than at 298 K. The decline in this ratio may be related to the decrease in the overlap of the third absorption with the lower energy absorptions of $Os_3(CO)_{12}$ at the lower temperature.

While a similar ligand dependent competition between associative photosubstitution and photofragmentation is observed for 436-nm excitation into the low-energy tail of the first electronic absorption feature of $Os_3(CO)_{12}$ at 298 K,[72] excitation into overlapping higher energy absorptions is not ruled out. The first allowed electronic transition for $Os_3(CO)_{12}$ is expected to give only slight labilization of both metal–metal and metal–ligand bonding, in accord with the extremely low photoconversion efficiencies observed at 436 nm. The $10a_1'$ level (HOMO) is best described as a mixture of Os–CO π bonding, metal–metal framework bonding exclusively of metal $p_{x,y}$ character directed toward the cluster core, and Os–CO σ antibonding. The 16e′ level is predominantly of axial CO π^* character. The $10a_1' \rightarrow 16e'$ transition thus represents only a small decline in metal framework bonding and a significant redistribution of CO π^* character to the axial ligands. Thus, it is not surprising to find that little photoreactivity

(67) L'Eplattenier, F.; Calderazzo, F. *Inorg. Chem.* **1968**, *7*, 1290–1293.
(68) (a) Moss, J. R.; Graham, A. G. *J. Chem. Soc., Dalton Trans.* **1977**, 95–99. (b) Rushman, P.; van Buuren, G. N.; Shiralian, M.; Pomeroy, R. K. *Organometallics* **1983**, *2*, 693–694.
(69) Carter, W. J.; Kelland, J. W.; Okrasinski, J.; Warner, K. E.; Norton, J. R. *Inorg. Chem.* **1982**, *21*, 3955–3960.
(70) Motyl, K. M.; Norton, J. R.; Schauer, C. K.; Anderson, O. P. *J. Am. Chem. Soc.* **1982**, *104*, 7325–7327.
(71) Wuu, Y.-M.; Bentsen, J. G.; Brinkley, C. G.; Wrighton, M. S. *Inorg. Chem.* **1987**, *26*, 530–540. Cf. also the recent work concerning $Os(CO)_n(\eta^2$-alkene$)_{5-n}$ recently reported.
(72) Pöe, A. J.; Sekhar, C. V. *J. Am. Chem. Soc.* **1986**, *108*, 3673–3679.

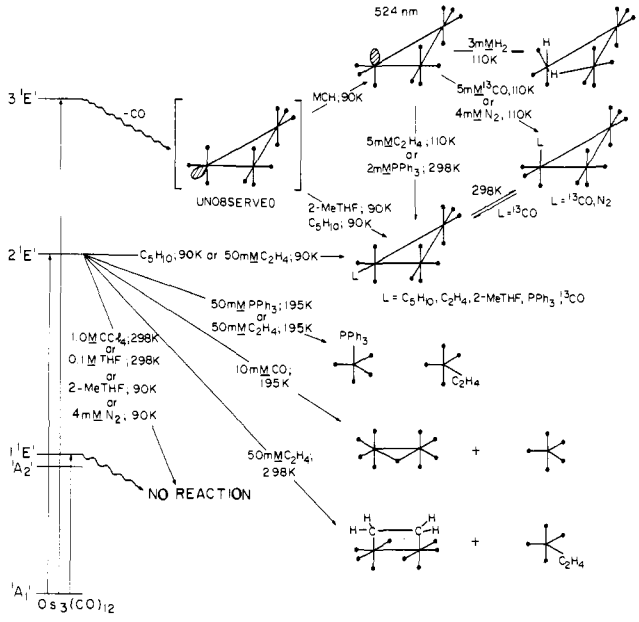

Figure 4. Summary of the wavelength dependent photoreaction chemistry observed for $Os_3(CO)_{12}$ in fluid solutions and in low-temperature hydrocarbon glasses. Excited state assignments are those from ref 38.

arises from selective excitation of the lowest energy allowed electronic transition for $Os_3(CO)_{12}$ at 90 K.

Conclusions

Figure 4 summarizes the wavelength-dependent photochemistry of $Os_3(CO)_{12}$. Our results suggest that the rates of internal conversion in $Os_3(CO)_{12}$ are only competitive with the rates of reaction from upper excited states. Excitation into the third absorption feature for $Os_3(CO)_{12}$ yields (i) dissociative loss of CO in an alkane glass at 90 K, (ii) substitution of CO by L (L = ^{13}CO, C_2H_4, C_5H_{10}, N_2, and 2-MeTHF) at 90 K, (iii) reaction with H_2 to form $H_2Os_3(CO)_{11}$ at 90 and at 298 K, and (iv) substitution of CO by PPh_3 and C_2H_4 at 298 K. No photochemistry is associated with the first electronic absorption of $Os_3(CO)_{12}$ at 90 K. However, excitation into the second electronic absorption yields associative substitution of CO by π-acids (^{13}CO, C_2H_4, C_5H_{10}), but not by N_2 or 2-MeTHF, at 90 K. In C_2H_4-, CO-, and PPh_3-containing fluid solutions at 195 and at 298 K, long wavelength excitation into the overlapping first and second electronic absorptions of $Os_3(CO)_{12}$ yields fragmentation products.

The 298 K photosubstitution quantum yield is $<10^{-4}$ for 436-nm excitation into the low-energy tail of the first absorption associated with the allowed electronic $10a_1' \rightarrow 16e'$ transition but increases at shorter wavelengths in correlation with an increasing contribution of absorption due to the third allowed electronic transition ($14e' \rightarrow 6a_2'$). The first allowed electronic transition of $Os_3(CO)_{12}$ is expected[38] to give only slight labilization of both metal–metal and metal–ligand bonding, in accord with the extremely inefficient cluster labilization observed with 436-nm excitation at 298 K and the lack of long wavelength photoreactivity ($\lambda > 370$ nm) at 90 K. Our results contrast with previous proposals[18] that the photochemistry of $Os_3(CO)_{12}$ is controlled by excitation into the first allowed electronic absorption and that internal conversion from the higher "$\sigma \rightarrow \sigma^*$ state" [associated with the second allowed electronic transition ($15e' \rightarrow 6a_2'$)] precludes observable photofragmentation.

Selective excitation into the second allowed electronic absorption ($15e' \rightarrow 6a_2'$; $\sigma \rightarrow \sigma^*$) of $Os_3(CO)_{12}$ is not possible in fluid solution, due to strongly overlapping higher energy features. However, the long wavelength photofragmentation pathway is consistent with the nature[38] of the second allowed electronic transition (absorption centered at 330 nm) as a transition from an orbital having strong metal–metal bonding contributions to one which is largely antibonding with respect to the metal–metal bonding framework of the cluster. Photofragmentation of $Os_3(CO)_{12}$ in the presence of excess CO was previously unobserved at 298 K in CH_3CN,[18] probably because of the known lability of the $Os(CO)_5$ and $Os_2(CO)_9$ photoproducts,[68] observed by us in alkane solution at 195 K, with respect to regeneration of $Os_3(CO)_{12}$. Detecting $Os(CO)_4(PPh_3)$ in low yield as an initial photoproduct of the long wavelength ($\lambda > 370$-nm) irradiation of $Os_3(CO)_{12}$ in PPh_3-containing solutions at 298 K was made possible by using sensitive FTIR detection, unavailable to the previous investigators.[18] The mononuclear products are, however, clearly detected in higher relative yield [with respect to competitive $Os_3(CO)_{11}(PPh_3)$ formation] during 195 K irradiation of similar solutions. This temperature dependence is most reasonably attributed to a decline in the contribution to the long wavelength absorption by the higher energy transition(s) associated with photosubstitution to form $Os_3(CO)_{11}(PPh_3)$. The second electronic absorption for $Os_3(CO)_{12}$ becomes well-resolved on further cooling to 90 K. Selective excitation into only the second absorption feature for $Os_3(CO)_{12}$ at 90 K yields associative substitution behavior. Photofragmentation efficiencies at 298 K and associative substitution efficiencies at 90 K are greater for strong π-acceptor ligands. While we have interpreted[19] similar photofragmentation results for $Ru_3(CO)_{12}$ in terms of a previously proposed[13,17] nonradical reactive isomer of the starting cluster and suggest the involvement of such an intermediate in the associative substitution of strong π-acceptors for CO at 90 K, excited state reactions of $M_3(CO)_{12}$ may also be important in rigid 90 K glasses, where fragmentation is suppressed, and in fluid solutions containing high concentrations of strong π-acceptor ligand.

After completing our work, Pöe and co-workers reported[72] the 436-nm photofragmentation and photosubstitution kinetics of reactions of $Os_3(CO)_{12}$ in benzene with 1-octene and $P(OEt)_3$. Consistent with our results in alkane media, they found that long wavelength photoreaction of $Os_3(CO)_{12}$ with 1-octene leads to fragmentation of the cluster whereas $P(OEt)_3$ gives associative substitution; both reactions proceed via a common intermediate proposed to be a nonradical reactive isomer of $Os_3(CO)_{12}$. Importantly, we propose that this intermediate is responsible for the long wavelength associative photosubstitution behavior observed for $Os_3(CO)_{12}$ at 90 K. This low-temperature photochemistry is associated with irradiation into the second electronic absorption for $Os_3(CO)_{12}$, a fact which is not in conflict with the observation of Pöe et al. for 436-nm excitation into the overlapping first and second electronic absorption of $Os_3(CO)_{12}$ at 298 K. Our results show that 366-nm irradiation into the second absorption (centered at 330 nm) of $Os_3(CO)_{12}$ yields photosubstitution of PPh_3 for CO with a quantum yield (much greater than that found for 436-nm irradiation) which is independent of PPh_3 or THF concentration, suggesting dissociative loss of CO as the mechanism for substitution at 298 K. These results differ from those of Pöe and co-workers at 436 nm, probably as a result of unavoidable excitation into the overlapping third allowed electronic absorption.

The wavelength-dependent photosubstitution quantum yields at 298 K and the wavelength-dependent accumulation of $Os_3(CO)_{11}$ at 90 K are most consistent with direct loss of CO only from an upper excited state. The dissociative loss of a nonstatistical excess of ^{12}CO ($^{12}CO/^{13}CO > 28$) from photoexcited, axial-^{13}CO–$Os_3(CO)_{11}(^{13}CO)$ suggests primary formation of equatorially vacant $Os_3(CO)_{11}$, Figure 4. The equatorially vacant $Os_3(CO)_{11}$ has not been detected and presumably isomerizes to an axially vacant $Os_3(CO)_{11}$ whose structure is suggested by the IR spectral features. The dissociation of equatorial CO from $Os_3(CO)_{12}$ is in keeping with the nature[38] of the third allowed electronic transition (absorption centered at 280 nm and tailing extensively to lower energy in fluid solution) as a transition ($14e' \rightarrow 6a_2'$; $\sigma^{*\prime} \rightarrow \sigma^*$) from an orbital having strong equatorial Os–CO π-back bonding to an orbital having strong equatorial M–CO σ antibonding. Importantly, we cannot rule out internal conversion to the dipole-forbidden HOMO–LUMO state, predicted[38] to facilitate Os–CO dissociative processes.

Equatorially vacant $Os_3(CO)_{11}$ rapidly isomerizes to the electronically favored axially vacant form with maintenance of a ligand array related to the anticuboctahedral ligand array of $Os_3(CO)_{12}$[49]

by removal of one CO. Low-temperature accumulation of axial-^{13}CO-$Os_3(CO)_{11}(^{13}CO)$ is consistent with the IR spectral characterization of the accumulated $Os_3(CO)_{11}$ precursor as an axially vacant fragment. The low-temperature reaction of axially vacant $Os_3(CO)_{11}$ with ^{13}CO to yield axial-^{13}CO-$Os_3(CO)_{11}(^{13}CO)$ has provided an opportunity to characterize the two possible isomers of $Os_3(CO)_{11}(^{13}CO)$.

Electronic factors are likely to control the thermodynamic preference for an axial vacancy in $Os_3(CO)_{11}$. The axial Os-CO bonds in $Os_3(CO)_{12}$[49] are lengthened relative to the equatorial Os-CO bonds due to a greater competition between two axial CO's than between an equatorial CO and a *trans*-Os atom for back donation of electron density from the t_{2g} orbitals of a given Os. This trend in Os-CO bonding extends to the crystallographically characterized axially substituted $Os_3(CO)_{11}(NCMe)$,[50] where, in addition, the axial Os-CO distance trans to the MeCN is the shortest metal-ligand bond distance in the structure. The trans axial CO receives most of the back-donated electron density from the Os orbital, since it is in direct competition with the MeCN, which is a good σ-donor but a poor π-acceptor. For sterically nondemanding entering groups, substitution of CO by weak π-acceptor ligands (CNMe, NCMe, C_5H_5N)[43] favors an axial coordination site trans to CO rather than an equatorial site trans to an Os-Os bond, thus maximizing π bonding with the remaining CO ligands. A "vacancy", having no π-acceptor properties, is similarly expected to reside in an axial site in photogenerated $Os_3(CO)_{11}$, as observed. The $Os_3(CO)_{11}(N_2)$ complex is axially substituted in accord with this trend. The strong π-acid C_2H_4, however, prefers to coordinate equatorially.

Acknowledgment. We thank the National Science Foundation for support of this research.

Registry No. $Os_3(CO)_{12}$, 15696-40-9; $Os_3(CO)_{11}$, 108345-48-8; $Os_3(CO)_{11}(PPh_3)$, 30173-88-7; $Os_3(CO)_{11}(P(OMe)_3)$, 66098-55-3; $Os(CO)_4(PPh_3)$, 21192-24-5; $Os_3(CO)_{11}(N_2)$, 108345-49-9; $Os_3(CO)_{11}(C_2H_4)$, 65772-73-8; $Os_3(CO)_{11}$(2-MeTHF), 108345-50-2; $Os_3(CO)_{11}(C_5H_{10})$, 108345-51-3; $H_2Os_3(CO)_{10}$, 41766-80-7; $H_2Os_3(CO)_{11}$, 56398-24-4; $Os_3(CO)_{11}(^{13}CO)$, 15696-40-9; axial-$Os_3(CO)_{11}(^{13}CO)$, 73346-54-0; equitorial-$Os_3(CO)_{11}(^{13}CO)$, 73295-94-0; $P(OMe)_3$, 121-45-9; PPh_3, 603-35-0; 2-MeTHF, 96-47-9; ^{13}CO, 1641-69-6; CO, 630-08-0; C_2H_4, 74-85-1; N_2, 7727-37-9; H_2, 1333-74-0; 1-pentene, 109-67-1.

Supplementary Material Available: IR and UV-vis spectral data for relevant complexes to supplement Table I and figures showing IR spectral data for the thermal reactions of photogenerated $Os_3(CO)_{11}$ with PPh_3 and with H_2 (6 pages). Ordering information is given on any current masthead page.

Wavelength-, Medium-, and Temperature-Dependent Competition between Photosubstitution and Photofragmentation in $Ru_3(CO)_{12}$ and $Fe_3(CO)_{12}$: Detection and Characterization of Coordinatively Unsaturated $M_3(CO)_{11}$ Complexes

James G. Bentsen and Mark S. Wrighton*

Contribution from the Department of Chemistry, Massachusetts Institute of Technology, Cambridge, Massachusetts 02139. *Received July 8, 1986*

Abstract: Irradiation of 0.1 mM $Ru_3(CO)_{12}$ (λ = 313 nm) or 0.02 mM $Fe_3(CO)_{12}$ (λ = 366 nm) in a methylcyclohexane or 2-methyltetrahydrofuran (2-MeTHF) glass at 90 K yields loss of one CO as the only IR detectable photoreaction to yield products formulated as $M_3(CO)_{11}$ or $M_3(CO)_{11}$(2-MeTHF), respectively. An initially observed axially vacant form of $Ru_3(CO)_{11}$ (II) having no bridging CO's rearranges at 90 K to an axially vacant form (III), having at least one bridging CO, also adopted by $Fe_3(CO)_{11}$ in an alkane glass. An initially observed, equatorially substituted form of $Ru_3(CO)_{11}$(2-MeTHF) (I') rearranges at 90 K to III or a 2-MeTHF adduct of III. I' is extremely photosensitive with respect to further substitution by 2-MeTHF for up to three CO ligands. $Ru_3(CO)_{11}$ (III) reacts with N_2 or ^{13}CO to yield $Ru_3(CO)_{11}(N_2)$ or axial-^{13}CO-$Ru_3(CO)_{11}(^{13}CO)$ complexes, respectively. $Ru_3(CO)_{11}$ and $Fe_3(CO)_{11}$ react with C_2H_4 to yield $M_3(CO)_{11}(C_2H_4)$ complexes. $M_3(CO)_{11}$ (III) reacts with PPh_3 to yield $Ru_3(CO)_{11}(PPh_3)$ at 298 K and $Fe_3(CO)_{11}(PPh_3)$ at 195 K. Long wavelength excitation of $Ru_3(CO)_{12}$ (λ = 366 nm) or $Fe_3(CO)_{12}$ (λ = 436 nm) yields negligible photochemistry in alkane or 2-MeTHF glasses but yields associative photosubstitution of C_2H_4, C_5H_{10}, and ^{13}CO but not N_2 or 2-MeTHF for CO at 90 K. Long wavelength ($\lambda > 540$ nm) excitation of $Fe_3(CO)_{12}$ yields no photochemistry at 90 K but gives asymmetric fragmentation in C_2H_4-containing alkane solutions at 298 K to yield 1 equiv each of $Fe(CO)_5$, $Fe(CO)_4(C_2H_4)$, and $Fe(CO)_3(C_2H_4)_2$; competitive photosubstitution occurs in the presence of PPh_3 to yield $Fe_3(CO)_{11}(PPh_3)$. At 195 K, the $Fe_3(CO)_{11}L/Fe(CO)_{5-n}(L)_n$ (L = C_2H_4, PPh_3; n = 0-2) product ratios increase with decreasing irradiation wavelength. Long wavelength ($\lambda > 420$ nm) irradiation of 0.2 mM $Ru_3(CO)_{12}$ in 195 K alkane solutions containing excess L = CO or C_2H_4 initially yields 1 equiv each of $Ru(CO)_4L$ and $Ru_2(CO)_8L$; $Ru_2(CO)_8(C_2H_4)$ fragments at 195 K to yield 2 more equiv of $Ru(CO)_4(C_2H_4)$. Long wavelength irradiation of $Ru_3(CO)_{12}$ in PPh_3-containing solutions at 195 K yields conversion to a CO-bridged product which reacts thermally at 195 K to form $Ru_3(CO)_{11}(PPh_3)$, in competition with $Ru_3(CO)_{12}$ regeneration; $Ru(CO)_4(PPh_3)$ and $Ru(CO)_3(PPh_3)_2$ are only observed as secondary photoproducts at 195 K. The low-temperature photochemistry of $Ru_3(CO)_{12}$ is discussed in terms of a wavelength-dependent competition between dissociative loss of equatorial CO from higher energy excitation and generation of a nonradical, reactive isomer of $Ru_3(CO)_{12}$ from long wavelength excitation. Implications of the new results for the photocatalyzed isomerization of 1-pentene to *cis*- and *trans*-2-pentene by $M_3(CO)_{12}$ (M = Ru, Fe) precursors are discussed.

This article reports results concerning the photochemical generation of reactive intermediates from visible and near-UV irradiation of $M_3(CO)_{12}$ (M = Fe, Ru) in low-temperature fluid solutions and in rigid organic solvents. A wavelength, medium, and temperature dependent competition between dissociative loss of CO and fragmentation enables selective photogeneration of coordinatively unsaturated $M_3(CO)_{11}$ (M = Fe, Ru) fragments with near-UV irradiation of $M_3(CO)_{12}$ in methylcyclohexane glasses according to eq 1 or, alternatively, reactive dinuclear Ru adducts of π-acceptor ligands (L = CO and C_2H_4) but not PPh_3 with visible light irradiation of $Ru_3(CO)_{12}$ in low-temperature alkane solutions according to eq 2.

0002-7863/87/1509-4530$01.50/0